Marine Pollution Bulletin 105 (2016) 7–22

Contents lists available at ScienceDirect

Marine Pollution Bulletin

journal homepage: www.elsevier.com/locate/marpolbul

Review

Weathering of field-collected floating and stranded Macondo oils during and shortly after the Deepwater Horizon oil spill

Scott A. Stout [a,*], James R. Payne [b], Stephen D. Emsbo-Mattingly [a], Gregory Baker [c]

[a] NewFields Environmental Forensics Practice, LLC, 300 Ledgewood Pl., Suite 305, Rockland, MA, United States
[b] Payne Environmental Consultants, Inc., 1651 Linda Sue Lane, Encinitas, CA, United States
[c] NOAA, Assessment and Restoration Division, 345 Middlefield Rd., MS-999, Menlo Park, CA, United States

ARTICLE INFO

Article history:
Received 23 December 2015
Accepted 18 February 2016
Available online 28 February 2016

Keywords:
Oil spill
Weathering
Polycyclic aromatic hydrocarbons
Biomarkers
Photo-oxidation

ABSTRACT

Chemical analysis of large populations of floating (n = 62) and stranded (n = 1174) Macondo oils collected from the northern Gulf of Mexico sea surface and shorelines during or within seven weeks of the end of the Deepwater Horizon oil spill demonstrates the range, rates, and processes affecting surface oil weathering. Oil collected immediately upon reaching the sea surface had already lost most mass below n-C_8 from dissolution of soluble aliphatics, monoaromatics, and naphthalenes during the oil's ascent with further reductions extending up to n-C_{13} due to the onset of evaporation. With additional time, weathering of the floating and stranded oils advanced with total PAH ($TPAH_{50}$) depletions averaging 69 ± 23% for floating oils and 94 ± 3% for stranded oils caused by the combined effects of evaporation, dissolution, and photo-oxidation, the latter of which also reduced triaromatic steroid biomarkers. Biodegradation was not evident among the coalesced floating oils studied, but had commenced in some stranded oils.

Contents

1. Introduction

Crude oil released (April 20 to July 15, 2010) from the Macondo well at a water depth of 1544 m following the explosion of the Deepwater Horizon (DWH) drill rig experienced different environmental fates. Some fraction of the crude oil released remained within the deep ocean as both a dissolved phase and as physically or chemically-dispersed, neutrally buoyant droplets that were transported laterally for several hundred kilometers at depths of ~1000 to 1300 m (Camilli et al., 2010; Hazen et al., 2010; Ryerson et al., 2012; Payne and Driskell, 2015a). Buoyancy forces caused another fraction of the oil to

* Corresponding author.
E-mail address: sstout@newfields.com (S.A. Stout).

http://dx.doi.org/10.1016/j.marpolbul.2016.02.044
0025-326X/

ascend through the water column. The surfaced oil formed multiple floating surface slicks, mousses, and sheens (Fig. S-1) that were spread by wind and currents over vast areas of the northern Gulf of Mexico (GoM) during the 87-day spill, before dissipating five weeks after the well was capped on July 15 (Ramseur, 2010).

Some fraction of floating Macondo oil became "stranded" on shorelines across the northern GoM. The first oil reached shorelines in Louisiana on approximately May 15, 2010 and about two weeks later in Mississippi, Alabama, and Florida (OSAT, 2011). It produced a highly visible and publicized impact on more than 1000 km of the region's beaches and marshes during the spring and summer of 2010 (Michel et al., 2013). This stranded oil was sometimes observed as "pure" viscous emulsions but more often as oil–mineral (sand) aggregates including tarballs (<10 cm), patties (10–50 cm), and oil mats (>50 cm) and as oily coatings on rocks, vegetation, shell hash, and wildlife (Fig. S-2).

All forms of floating and stranded Macondo oil had undoubtedly experienced chemical changes compared to the fresh Macondo oil due to progression in the natural weathering processes (dissolution, evaporation, biodegradation and/or photo-oxidation) during its ascent through the water column, transport while at the sea surface, and after arriving at shorelines. In addition to natural weathering processes, some fraction of the floating oil was treated with chemical dispersants in an effort to disperse the oil into the water column as a means to enhance the natural weathering processes.

Determining the chemical changes brought about by weathering of the floating and stranded Macondo oil during and immediately following the DWH oil spill is critical for understanding its potential ecological and toxic effects on natural resources in or near the sea surface (e.g., marine mammals, turtles, sea birds, fish and fish embryos, and plankton) and on the region's shoreline ecosystems. Earlier studies reported on the composition of small numbers of floating and/or stranded Macondo oils collected during the active spill or shortly thereafter (Aeppli et al., 2012, 2014; Liu et al., 2012; Carmichael et al., 2012; Kiruri et al., 2013; Hall et al., 2013; McKenna et al., 2013; Lewan et al., 2014; Ruddy et al., 2014; Faksness et al., 2015). These studies collectively showed the floating and stranded oils experienced molecular level changes consistent with varying degrees of evaporation, dissolution and/or photo-oxidation, although biodegradation of the surfaced oil was not obvious in the weeks following the spill. The largest study reported on the compositions of 17 floating oils and four sand patties collected during the active spill, which exhibited decreases in volatile compounds consistent with evaporation and increases in the percent mass of oxygen-containing moieties that the authors originally attributed to the combined effects of biodegradation and photo-oxidation (Aeppli et al., 2012). Subsequent studies of field-collected oils during the spill also reported on the increase in polar, mostly oxygenated and non-chromatographable species accompanying weathering (Hall et al., 2013; Kiruri et al., 2013; McKenna et al., 2013; Lewan et al., 2014; Aeppli et al., 2014; Ruddy et al., 2014), which based upon laboratory photo-degradation studies (Lewan et al., 2014; King et al., 2014; Radović et al., 2014), were attributed to the rapid photo-oxidation of the spilled oil under the high insolation conditions of the northern GoM.

Although informative as to the chemical changes and weathering processes at work, none of these earlier studies necessarily captured the full range of weathering of the surfaced oil during and shortly following the DWH spill owing to the limited numbers of samples studied. In addition, molecular level changes in polycyclic aromatic hydrocarbons (PAHs), compounds conventionally linked to potential ecological and toxic effects on natural resources, were not fully quantified.

In this study, we report on the chemical characteristics of large populations of floating (62) and stranded Macondo oils (1174) collected during and shortly after the DWH spill as part of the Trustees Natural Resource Damage Assessment (NRDA). The objective is to reveal the range in composition of the surface oil, particularly PAHs, ranging from the time when oil first reached the sea surface to when it was found stranded over approximately 800 km of northern GoM shorelines within about seven weeks after the spill ended. The "least" and "most" weathered floating and stranded oils from these large sample populations provide a basis to evaluate the full range in oil composition to which near surface and shoreline natural resources were exposed during and shortly after the DWH oil spill. Compositions of these large populations of authentic field collected samples are also (1) useful for establishing the spatial extent of Macondo oil on the region's shorelines through chemical analysis (e.g., as a supplement to remote sensing or SCAT observations), (2) provide a real-world assessment of the full range of weathering in field-collected samples that can be compared to laboratory- or model-predicted compositions of floating and stranded oils, (3) provide a baseline against which longer-term (post-2010) weathering studies of Macondo oil in the northern GoM might be compared, and (4) provide a basis to compare weathering following the DWH spill to past and future spills.

2. Materials and methods

2.1. Field-collected samples and fresh Macondo oil

A population of 62 floating Macondo oil samples – slicks, sheens, and mousses – was collected between May 10 and July 29, 2010, i.e., 20 to 100 days after the spill started on April 20, 2010. Sixty floating oil samples were collected before June 20 and during the active spill and two samples were collected between 4 and 14 days after the spill was stopped on July 15, 2010. The samples were collected between about 1.5 and 69 km from the Macondo wellhead, but mostly less than 25 km and north of the wellhead (Fig. 1). No samples were collected less than 1.5 km from the wellhead due to restrictions on NRDA vessels accessing this area during the active spill. All 60 of the floating oil samples collected during the active spill were collected using pre-cleaned TFE-fluorocarbon nets (ASTM D4489) attached to fishing or telescoping poles from the sides of ships. Upon retrieval the oiled nets were placed back into pre-cleaned glass jars for shipment to the laboratory. The two floating oil samples collected after the active spill were aliquots collected by response vessels equipped with mechanical skimmers.

The population of 1174 stranded Macondo oils – tarballs, patties, oil mats, oiled vegetation, TFE-fluorocarbon nets (to collect liquid oil or to wipe oil coatings from solid surfaces) and oiled debris (wood and plastic) – was collected from the supra-tidal and intertidal portions of shorelines in Louisiana, Alabama, Mississippi, and Florida between May 24 and September 2, 2010, i.e., 34 to 135 days after the spill began on April 20, 2010 and up to 7 weeks after the spill ended on July 15, 2010. (Notably, 114 additional stranded oil samples were collected and analyzed, but determined through chemical fingerprinting to be comprised of non-Macondo oils; these are not discussed further in this paper.) The stranded oil samples spanned approximately from western Terrebonne Bay, Louisiana to St. Vincent Sound, Florida, and included numerous offshore islands (Fig. 1). The stranded oil samples were collected by teams of NRDA researchers by walking shorelines or by wading ashore from small boats.

Given the large number of samples and volume of data collected, for this study the range of weathering found among the 62 floating and 1174 stranded oil studies is represented by focusing on four samples considered to be the representatives of the "least" and "most" weathered floating and stranded oils studied, respectively (Table 1). Not surprisingly the "least" weathered floating oil was collected within seconds of reaching the sea surface as finite oil droplets were observed to surface in open water and "burst" to spread into rainbow-colored and silver sheens; whereupon the rainbow sheen was immediately sampled by one of the authors (JRP; Fig. S-3). This sample exhibits weathering experienced during the oil's ascent to the surface and/or immediately after surfacing (Table 1). The "least" weathered stranded oil was collected from an approximately 6 m long, black oil slick as it arrived at a marsh edge in the eastern birdfoot region of Louisiana about 80 km from the Macondo well (Table 1). These two "least" weathered samples

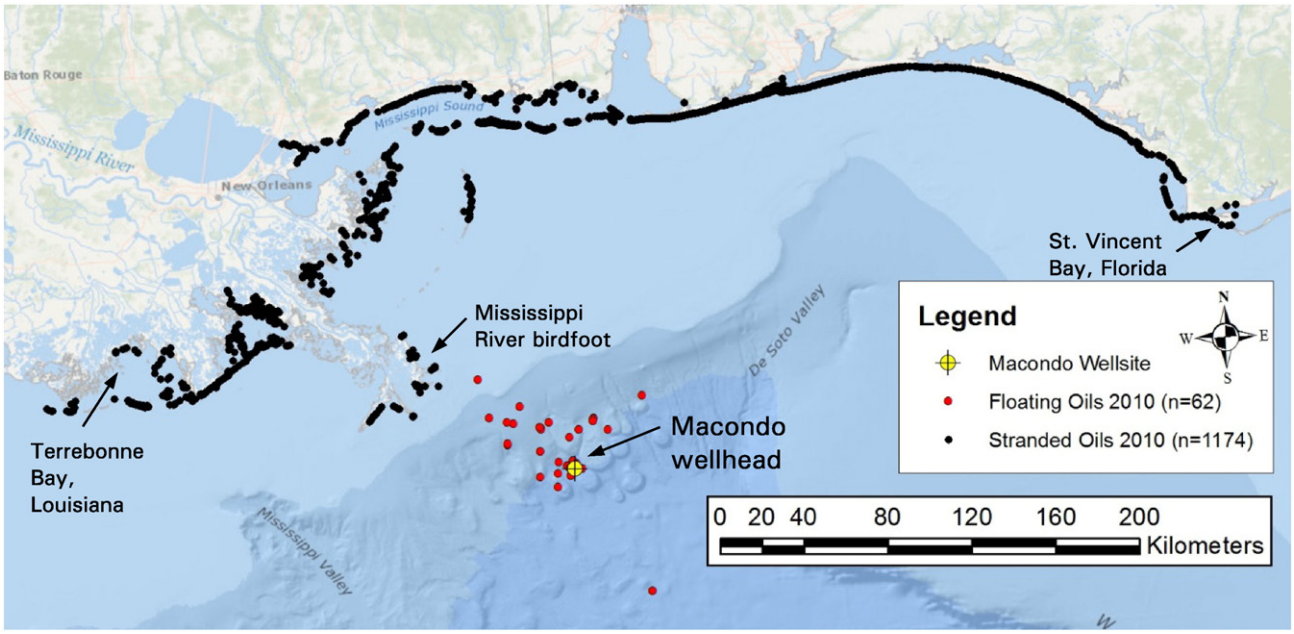

Fig. 1. Map showing the location of 62 floating oil and 1174 stranded Macondo oil samples collected in 2010 following the Deepwater Horizon oil spill.

are highlighted herein since they reflect the character of the "freshest" oils to which near surface and shoreline resources, respectively, were exposed during the DWH spill. The "most" weathered floating and stranded oils highlighted reflect the maximum degrees to which weathering altered the composition of the oil while it was still floating offshore or after reaching shore, respectively.

These least and most weathered samples' results are compared to unweathered Macondo oil, which is represented by the average results of six samples collected on May 21, 2010 on the drillship Discoverer Enterprise from the riser insertion tube that was receiving oil directly from the well's broken riser near the sea floor. Six 2.5 L liquid oil samples (bottles 1 to 5 and 71) were collected in sequence at ambient temperature and pressure, i.e., no attempt was made to preserve any exsolving gas fraction as the oil reached ambient conditions. These samples were determined to be unadulterated and contain no additives (e.g., Nalco EC9323A defoamer). The average results for these six oils, analyzed in two analytical batches, were used herein to represent unweathered Macondo oil.

All of the oil samples were stored on ice (<4 °C) immediately after collection and then frozen before being shipped cold to Alpha Analytical Laboratory (Alpha; Mansfield, Massachusetts) under full chain-of-custody procedures. Upon receipt at the laboratory all samples were stored in the dark and frozen (−20 °C) prior to sample preparation and instrument analysis.

2.2. Sample preparation

Floating oil (net) samples were spiked with recovery internal surrogates (RIS; 5α-androstane, acenaphthene-d_{10}, chrysene-d_{12}) and serially-extracted (3×) using fresh dichloromethane (DCM) on a shaker table. The extracts were combined, passed through glass wool, dried with sodium sulfate, concentrated to 1 ml, and spiked with surrogate internal standards (SIS; *o*-terphenyl, *n*-tetracosane-d_{50}, 2-methylnaphthalene-d_{10}, pyrene-d_{10}, benzo(b)fluoranthene-d_{12}, and 5β(H)-cholane) prior to instrument analysis. Most stranded oil samples (and the two larger volume floating oils) were diluted in DCM and then processed through a glass fiber filter and anhydrous Na_2SO_4 to remove sand and water, respectively. A 1 mL aliquot of the filtered extract was then spiked with SIS and RIS prior for instrument analysis. The stranded oil from nets, vegetation, and other debris was rinsed from their surface using DCM and concentrated. A 1 mL aliquot was spiked with SIS and RIS for instrument

Table 1
Inventory of the least and most weathered floating and stranded Macondo oil samples among the large populations studied.

Sample ID	Alpha lab ID	Sample date	Description
Fresh Macondo oils			
GU2988-A0521-O9801	1005074-01	21-May-10	Liquid (dead) oil collected by riser insertion tube to Discoverer Enterprise
GU2988-A0521-O9802	1005074-04	21-May-10	
GU2988-A0521-O9803	1005074-02	21-May-10	
GU2988-A0521-O9804	1005074-05	21-May-10	
GU2988-A0521-O9805	1005074-03	21-May-10	
GU2988-A0521-O9871	1009311-01	21-May-10	
Floating Macondo oils			
JF3-2 km-onet-20100616-surf-N143	1007189-14	16-Jun.-10	Sheen collected immediately upon surfacing; 2 km north of well. Representative of the "least" weathered floating oil studied.
GU-10-02-005-T-003	1007190-13	30-May-10	Sheen collected 19 km north of well. Representative of the "most" weathered floating oils studied.
Stranded Macondo oils			
LAAQ43-B0528-4902	1209049-06	28-May-10	Stranded black oil; 80 km from well in eastern Bird Foot area, Louisiana. Representative of "least" weathered stranded oil studied.
LAAR37-A0820-B116002	1008280-02	20-Aug.-10	Stranded tarball; 200 km from well in eastern Timbalier Bay, Louisiana. Representative of the "most" weathered stranded oil studied.

analysis. The unweathered Macondo oils (50 mg) were diluted in DCM, concentrated to 1 mL and spiked with SIS and RIS. No silica-gel cleanup of the sample extracts was performed.

Each analytical batch of authentic samples (n < 20) included a procedural blank (PB; 1 mL of DCM), a laboratory control sample (LCS) and LCS duplicate (LCSD), each consisting of 1 mL of DCM spiked with selected hydrocarbons in known concentrations to monitor method accuracy, a NIST 1582 crude oil standard reference material, and one sample duplicate (i.e., a single oil prepared twice) as a measure of precision and reproducibility of the data.

2.3. Instrument analysis

All sample extracts were analyzed using a (1) modified EPA Method 8015B and (2) modified EPA Method 8270 as described in the following paragraphs. Additional details of these methods are described elsewhere (Douglas et al., 2015).

Modified EPA Method 8015B was conducted via gas chromatography-flame ionization detection (GC-FID; Agilent 6890) equipped with a Restek Rtx-5 (60 m × 0.25 mm ID, 0.25 μm film) fused silica capillary column. Extracts were injected (1 μL, pulsed splitless) into the GC programmed from 40 °C (1 min) and ramped at 6 °C/min to 315 °C (30 min) using H_2 (~1 mL/min) as the carrier gas. This analysis was used to determine the concentrations of GC-amenable total extractable material (TEM; C_9–C_{44}) and individual *n*-alkanes (C_9–C_{40}) and (C_{15}–C_{20}) acyclic isoprenoids (Table 2). Prior to sample analysis a minimum five-point calibration was performed to demonstrate the linear range of the analysis. The calibration solution was composed of selected aliphatic hydrocarbons within the *n*-C_9 to *n*-C_{40} range. Analyte concentrations in the standard solutions ranged from 1 ng/μL to 200 ng/μL. Target analytes that were not in the calibration solution had the average response factor (RF) of the nearest eluting compound(s) assigned as follows: RF of *n*-C_{14} assigned to C_{15} isoprenoids, *n*-C_{15} assigned to C_{16} isoprenoids; *n*-C_{17} assigned to nor-pristane, and *n*-C_{40} assigned to *n*-C_{39}. All calibration solution compounds that fall within the window were used to generate the average RF for TEM. TEM was quantified by integrating the total C_9–C_{44} area after blank subtraction. Calibration check standards representative of the mid-level of the initial calibration and the instrument blank were analyzed every 10 samples. The check standard's response was compared versus the average RF of the respective analytes contained in the initial calibration. All authentic samples and quality control samples were bracketed by passing mid-check standards.

Modified EPA Method 8270 was conducted via gas chromatography–mass spectrometry (GC–MS; Agilent 7890 GC with 5975c MS) with the MS operated in the selected ion monitoring (SIM) mode for improved sensitivity. Extracts were injected (1 μL, pulsed splitless) into the GC containing a 60 m × 0.25 mm ID, 0.25 μm film, Phenomenex ZB-5 capillary column and the oven programmed from 35 °C (1 min) and

Table 2
Concentrations of *n*-alkanes, isoprenoids, and TEM in fresh, floating, and stranded Macondo crude oils. Concentrations are μg/g_{oil}.

	Fresh Macondo oil		Floating Macondo oils				Stranded Macondo oils			
Saturated hydrocarbons (μg/g_{oil})	Average (n = 6)	StDev	Average (n = 62)	StDev	Least weathered[a]	Most weathered[b]	Average (n = 1174)	StDev	Least weathered[c]	Most weathered[d]
n-Nonane (C9)	10,100	816	209	422	1454	5	4	8	1	nd
n-Decane (C10)	8870	890	422	987	4094	3	6	7	6	nd
n-Undecane (C11)	8510	773	772	1614	7047	4	4	5	3	nd
n-Dodecane (C12)	7610	682	1216	2044	8482	5	7	8	8	nd
n-Tridecane (C13)	7020	640	1970	2395	8372	6	11	29	103	nd
2,6,10 Trimethyldodecane (1380)	1400	112	496	541	1665	5	2	12	89	nd
n-Tetradecane (C14)	6250	603	2502	2615	7461	7	12	41	754	5
2,6,10 Trimethyltridecane (1470)	2260	301	1126	1040	2723	13	16	37	634	4
n-Pentadecane (C15)	6310	784	3895	3364	8455	51	70	151	2279	21
n-Hexadecane (C16)	5230	538	3724	2735	6228	206	235	336	3827	30
Norpristane (1650)	1610	199	1308	819	1960	141	165	180	1972	159
n-Heptadecane (C17)	4380	481	4140	2235	5906	642	772	644	5417	87
Pristane	2920	267	2554	1350	3514	446	534	404	3339	613
n-Octadecane (C18)	3570	474	4031	1485	4444	1270	1693	844	5692	254
Phytane	1570	107	1779	568	2033	599	822	368	2459	984
n-Nonadecane (C19)	3190	340	4057	903	3956	2190	2772	942	5639	407
n-Eicosane (C20)	2990	393	4250	631	3910	3130	3830	945	5629	583
n-Heneicosane (C21)	2500	226	3651	430	3137	3350	3882	853	4791	506
n-Docosane (C22)	2370	210	3414	400	2843	3550	3868	816	4367	489
n-Tricosane (C23)	1860	176	2884	338	2355	3230	3412	732	3625	400
n-Tetracosane (C24)	1710	163	2668	334	2153	3120	3220	744	3328	426
n-Pentacosane (C25)	1690	305	2562	330	1987	2910	3050	607	2968	808
n-Hexacosane (C26)	1330	114	2044	263	1573	2440	2583	541	2650	681
n-Heptacosane (C27)	1040	103	1666	214	1279	1990	1957	430	1993	544
n-Octacosane (C28)	761	85	1293	173	984	1590	1597	429	2109	386
n-Nonacosane (C29)	713	83	1286	207	929	1710	1531	346	1622	473
n-Triacontane (C30)	653	70	1083	168	719	1420	1385	289	1367	499
n-Hentriacontane (C31)	574	48	1080	204	655	1500	1372	274	1367	616
n-Dotriacontane (C32)	549	62	916	204	464	1250	1191	218	1092	528
n-Tritriacontane (C33)	367	42	685	176	294	993	1012	186	1008	546
n-Tetratriacontane (C34)	297	50	577	155	213	775	878	188	790	515
n-Pentatriacontane (C35)	240	33	497	144	189	675	731	136	694	410
n-Hexatriacontane (C36)	209	63	377	130	112	445	560	117	544	283
n-Heptatriacontane (C37)	148	29	309	128	70	319	464	100	440	186
n-Octatriacontane (C38)	141	32	289	125	67	245	432	98	402	198
n-Nonatriacontane (C39)	108	18	245	137	35	140	320	93	259	138
n-Tetracontane (C40)	100	17	226	132	38	115	303	95	233	99
Total extractable material (TEM)	681,000	52,400	601,144	93,437	736,920	518,000	588,666	84,939	693,240	464,000

[a] JF3-2 km-onet-20,100,616-surf-N143.
[b] GU-10-02-005-T-003.
[c] LAAQ43-B0528-BA4902.
[d] LAAR37-A0820-B116002 (see Table 1).

Table 3
Concentrations of PAH analytes and hopane in fresh, floating, and stranded Macondo crude oils. Concentrations are $\mu g/g_{oil}$.

Abbrev	Analytes	Fresh Macondo oil		Floating Macondo oils				Stranded Macondo oils			
		Average (n = 6)	StDev	Average (n = 62)	StDev	Least weathered[a]	Most weathered[b]	Average (n = 1174)	StDev	Least weathered[c]	Most weathered[d]
D0	cis/trans-Decalin	779	43	38	85	326	0.1	0.1	0.4	nd	0.2
D1	C1-Decalins	1174	56	89	175	697	nd	0.1	0.9	nd	nd
D2	C2-Decalins	966	36	117	196	735	nd	0.1	1.2	nd	nd
D3	C3-Decalins	436	13	82	115	418	nd	0.1	1.0	nd	nd
D4	C4-Decalins	431	29	125	137	410	nd	0.3	2.8	43	nd
BT0	Benzothiophene	7.3	0.6	0.8	1.5	5.8	nd	0.003	0.05	nd	nd
BT1	C1-Benzo(b)thiophenes	33	1.2	6.6	7.4	29	nd	0.1	0.7	nd	nd
BT2	C2-Benzo(b)thiophenes	31	1.9	9.0	8.9	31	nd	0.8	2.1	5.4	nd
BT3	C3-Benzo(b)thiophenes	48	3.8	20	18	51	nd	0.2	1.3	15	nd
BT4	C4-Benzo(b)thiophenes	37	0.4	20	16	38	nd	0.4	2.0	26	nd
N0	Naphthalene	964	68	31	80	346	0.2	0.3	0.5	0.2	0.4
N1	C1-Naphthalenes*	2106	123	234	416	1607	0.5	0.7	0.8	3.5	0.6
N2	C2-Naphthalenes*	2259	297	587	730	2371	1.3	2.5	6.3	118	1.6
N3	C3-Naphthalenes*	1597	63	609	597	1646	3.1	7.1	20	361	1.9
N4	C4-Naphthalenes*	721	25	363	303	752	7.5	14	24	348	6.5
B	Biphenyl	204	20	41	56	197	0.2	0.3	0.3	2.5	0.4
DF	Dibenzofuran	30	2.8	11	12	35	0.2	0.1	0.3	3.9	0.1
AY	Acenaphthylene	8.9	1.1	3.0	3.3	9	0.1	0.1	0.4	0.9	nd
AE	Acenaphthene	21	4.4	8.1	9.3	28	0.1	0.05	0.4	3.0	nd
F0	Fluorene	150	12	60	62	180	0.8	0.9	1.9	32	0.3
F1	C1-Fluorenes*	308	27	185	158	391	5.3	7.4	12	171	2.1
F2	C2-Fluorenes*	404	24	293	201	485	22	37	33	393	22
F3	C3-Fluorenes*	286	19	247	135	334	40	70	39	419	48
A0	Anthracene	2.3	6.3	3.9	5.8	nd	nd	0.5	1.2	11	0.5
P0	Phenanthrene	310	32	201	159	411	14	12	18	213	2.9
PA1	C1-Phenanthrenes/Anthracenes*	676	54	569	317	862	101	117	88.1	867	60
PA2	C2-Phenanthrenes/Anthracenes*	657	45	650	268	805	180	248	126.1	1149	193
PA3	C3-Phenanthrenes/Anthracenes*	381	19	355	142	412	98	150	74	676	144
PA4	C4-Phenanthrenes/Anthracenes*	148	12	150	62	176	40	68	30	269	69
RET	Retene	nd	nd	nd	nd	nd	nd	1.4	11	nd	nd
DBT0	Dibenzothiophene	53	6.8	33	28	69	1.5	1.6	2.5	32	0.4
DBT1	C1-Dibenzothiophenes*	153	16	128	79	202	16	22	19	192	17
DBT2	C2-Dibenzothiophenes*	197	18	199	85	245	51	76	38	371	59
DBT3	C3-Dibenzothiophenes*	146	14	162	57	178	53	83	34	306	80
DBT4	C4-Dibenzothiophenes*	72	5.2	80	28	86	29	50	19	174	51
BF	Benzo(b)fluorene	11	1.0	7.5	7.6	17	nd	0.1	0.7	9.4	nd
FL0	Fluoranthene	4.1	1.1	3.6	1.8	5.8	0.7	1.8	7.8	5.8	0.5
PY0	Pyrene	16	3.2	15	8.4	21	2.0	4.4	6.7	27	2.7
FP1	C1-Fluoranthenes/Pyrenes*	80	5.6	76	42	106	13	23	11	112	19
FP2	C2-Fluoranthenes/Pyrenes*	130	9.1	124	72	177	17	30	16	175	25
FP3	C3-Fluoranthenes/Pyrenes*	158	11	154	82	208	33	58	23	244	48
FP4	C4-Fluoranthenes/Pyrenes*	125	8.9	139	65	177	43	75	26	246	74
NBT0	Naphthobenzothiophenes	18	1.9	27	6	29	14	18	6	44	16
NBT1	C1-Naphthobenzothiophenes*	56	5.8	79	19	91	39	54	16	128	58
NBT2	C2-Naphthobenzothiophenes*	80	7.0	100	31	114	39	62	21	169	71
NBT3	C3-Naphthobenzothiophenes*	58	5.0	70	30	90	19	35	13	116	38
NBT4	C4-Naphthobenzothiophenes*	37	7.0	48	23	64	11	32	13	93	27
BA0	Benz[a]anthracene	7.3	1.6	5.0	3.8	7.6	nd	0.4	3.7	3.7	nd
C0	Chrysene/Triphenylene	56	5.4	68	13	64	40	59	13	98	57
BC1	C1-Chrysenes*	129	11	139	40	160	59	99	24	198	118
BC2	C2-Chrysenes*	158	16	153	67	194	43	78	24	191	104
BC3	C3-Chrysenes*	156	18	129	75	192	23	53	17	145	59
BC4	C4-Chrysenes*	90	12	77	50	113	15	38	11	94	40
BBF	Benzo[b]fluoranthene	6.1	0.9	7.4	1.4	6.8	4.4	6.4	3.9	11.4	7.0
BJKF	Benzo[jk]fluoranthene	0.5	1.0	0.04	0.2	nd	nd	0.3	3.4	nd	nd
BAF	Benzo[a]fluoranthene	0.7	0.2	nd	nd	nd	nd	0.1	0.8	nd	nd
BEP	Benzo[e]pyrene	12	1.2	14	4.4	15	5.3	8.8	3.8	19	9.1
BAP	Benzo[a]pyrene	3.2	0.8	2.4	1.8	3.8	nd	0.5	3.7	2.1	nd
PER	Perylene	1.0	0.3	0.8	0.8	1.4	nd	0.2	1.1	0.5	nd
IND	Indeno[1,2,3-cd]pyrene	1.2	0.7	0.6	0.8	1.2	nd	0.4	2.7	1.0	nd
DA	Dibenz[a,h]anthracene	2.5	0.8	1.9	1.3	2.6	nd	0.3	1.0	1.8	nd
GHI	Benzo[g,h,i]perylene	2.3	0.8	2.4	0.9	2.6	0.7	1.4	2.5	2.9	1.2
Hop	Hopane	68.8	4.8	112	16.1	81.0	144	143	22	130	136
$TPAH_{50}$	Σ 50 N0 to GHI, excl. RET and PER	13,300	507	6640	4140	13,700	1090	1708	746	8250	1540
$PetPAH_{27}$	Σ 27 analytes indicated by*	11,400	375	6100	3750	12,300	1000	1580	639	7230	1360
	$TPAH_{50}$ depletion	–	–	69	23	12	96	94	3	67	94
	$TPAH_{27}$ depletion	–	–	61	27	0	95	93	3	64	96

[a] JF3-2 km-onet-20,100,616-surf-N143.
[b] GU-10-02-005-T-003.
[c] LAAQ43-B0528-BA4902.
[d] LAAR37-A0820-B116002 (see Table 1).

ramped at 6 °C/min to 315 °C (30 min) using He as the carrier gas. This analysis was used to determine the concentrations of 62 parent and alkylated decalins, polycyclic aromatic hydrocarbons (PAH), sulfur-containing aromatics, and 54 petroleum biomarkers (i.e., tricyclic and pentacyclic triterpanes and steranes, and triaromatic steroids (Table 3). Prior to sample analysis, the GC–MS was tuned with perfluorotributylamine (PFTBA) at the beginning of each analytical sequence. A minimum 5-point initial calibration consisting of selected target compounds was established to demonstrate the linear range of the analysis. Analyte concentrations in the standard solutions ranged from 0.01 to 10.0 ng/μL for PAH and 0.01 to 20.0 ng/μL for biomarkers. Quantification of target compounds was performed by the method of internal standards using average response factor (RF) determined in the 5-point initial calibration. Alkylated PAHs were quantified using the RF of the corresponding parent, triterpanes were quantified using the RF's for 17α(H),21β(H)-hopane, and steranes and triaromatic steroids were quantified using the RF of 5β(H)-cholane. Biomarker identifications were based upon the comparison to selected authentic standards (Chiron Laboratories), elution patterns in the peer-reviewed literature, and mass spectral interpretation from full scan GC/MS analyses conducted at Alpha.

Aliquots of each sample extract were used to determine the gravimetric weight of the recoverable oil, thereby allowing the concentrations of target analytes to be reported on an oil weight basis ($\mu g/g_{oil}$). All sample locations and surrogate-corrected concentration data are publically available through NOAA Deepwater Horizon NRDA data portal, DIVER (Data Integration Visualization Exploration and Reporting), available at https://dwhdiver.orr.noaa.gov/. All concentrations used herein have been converted to non-surrogate values.

In addition to the modified EPA Methods described above, the unweathered Macondo oil was analyzed using high temperature simulated distillation (HTSD) via ASTM D7169 (Villalanti et al., 2000; Triton Analytics Corp., Houston, TX). This analysis measured the mass recovered over the temperature range of 35 to 750 °C (C_5 to C_{120}). Because TEM (described above) measures only GC-amenable mass between C_9 and C_{44}, the HTSD results were used to characterize the full boiling/carbon range distribution of the unweathered liquid (C_5+) oil and provide a basis to determine the non-GC amenable ($>C_{44}$) mass present in the oil.

2.4. Degree of weathering quantification

The degree of weathering in each of the floating and stranded Macondo oils was determined based upon the mass losses relative to the conservative internal marker within the oil, viz., 17α(H),21β(H)-hopane (hopane), which has proven recalcitrant to biodegradation (Prince et al., 1994) and photo-oxidation (Garrett et al., 1998). The percent depletion of any given fraction (e.g., total PAHs) or individual chemical (e.g., naphthalene) in the floating or stranded oils was estimated using the following formula:

$$\%\text{Depletion of A} = [((A_0/H_0)-(A_s/H_s))/(A_0/H_0)] \times 100 \quad (1)$$

where A_s and H_s are the concentrations of the target analyte and hopane in the weathered oil sample, respectively, and A_0 and H_0 are the concentrations of the target analyte and hopane in the average, fresh Macondo source oil. Although hopane can be degraded under some circumstances, if it (H_s) was reduced in a given field sample, any %depletions calculated for that sample would be underestimated.

3. Results and discussion

3.1. TEM, n-alkanes, and acyclic isoprenoids

The range of weathering among the floating and stranded Macondo oils during and shortly after the DWH spill is demonstrated by the least and most weathered samples among the large populations studied (Table 1). The GC-FID chromatograms for these samples and fresh Macondo oil are shown in Fig. 2 and the tabulated concentrations of TEM, acyclic isoprenoids, and *n*-alkanes for these representative samples, and for the average concentrations in the populations of floating and stranded Macondo oils studied, are given in Table 2.

The fresh Macondo oil is dominated by a series of *n*-alkanes that steadily decrease in concentration with increasing carbon number (Fig. 2A; Table 2). The GC-amenable fraction of the oil yielded a TEM (C_9–C_{44}) concentration of 681,000 μg/g (68.1 wt%; Table 2). This result is consistent with that determined by HTSD analysis which revealed approximately 20 wt% of the unweathered oil occurred in the C_5 to C_9

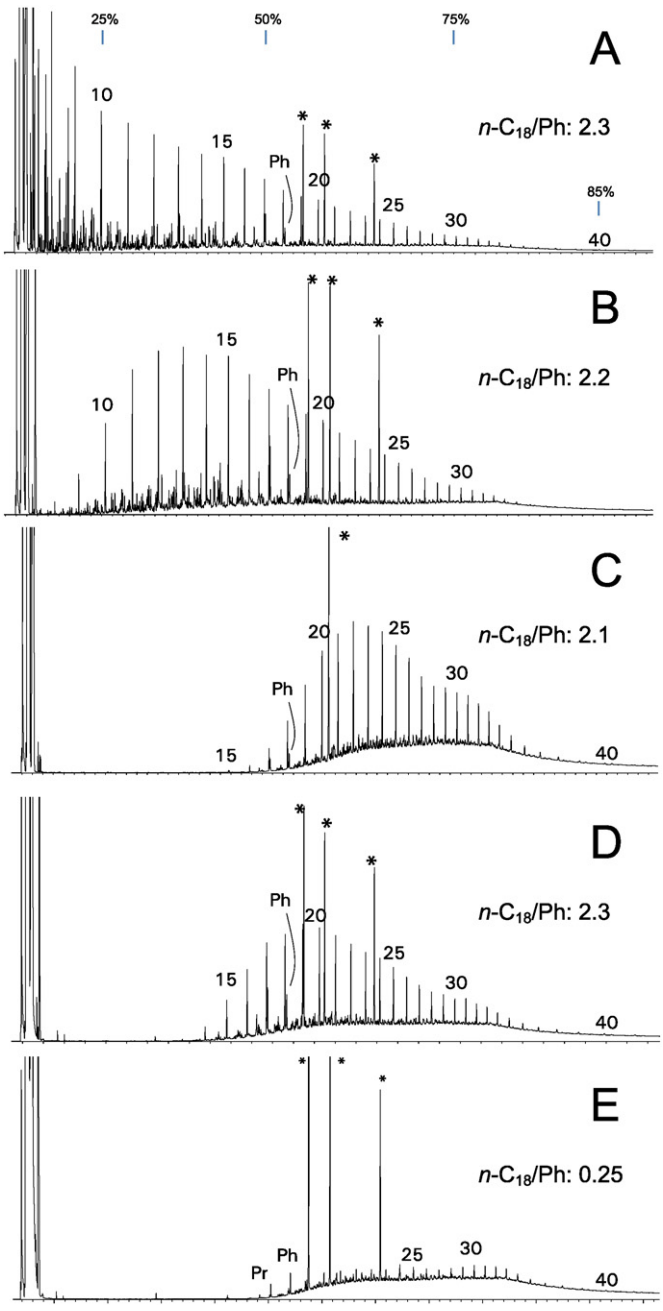

Fig. 2. GC-FID chromatograms exemplifying the range of weathering among floating and stranded Macondo oils in 2010. (A) Fresh Macondo oil, (B) least weathered floating oil, (C) most weathered floating oil, (D) least weathered stranded oil, and (E) most weathered stranded oil. Pr — pristane; Ph — phytane; # — *n*-alkane carbon number; * — internal. Standard. See Table 1 for sample descriptions. Percent mass of the liquid (C_5+) oil indicated by the HTSD results of fresh Macondo oil (Fig. S-3) is annotated in (A).

range and another 12 wt% was non-GC amenable and occurred above C_{44} (Fig. S-4; Table S-1).

The Macondo oil collected immediately after appearing at the sea surface shows a loss of nearly all compounds below n-C_8, with at least some reduction of all compounds below n-C_{13} (Fig. 2B). Based upon the HTSD results of the unweathered oil, this loss is estimated to be approximately 20 to 25 wt% of the oil. Included within this range are the BTEX compounds, which were not typically measured in our study. Some fraction of these highly soluble monoaromatics is known to have been dissolved into the water column during the oil's ~1500 m ascent to the sea surface (Hazen et al., 2010; Reddy et al., 2012). This is expected as similar dissolution of BTEX was observed in oil rising from a depth of only 60 m during the IXTOC I blowout in 1979 (Payne et al., 1980). During the DWH oil spill, however, at least some BTEX reached the sea surface as evidenced by its detection in air samples taken near the sea surface (NIOSH, 2010). BTEX and lower-molecular-weight aliphatics that were not dissolved during the oil's ascent are anticipated to have rapidly evaporated (Jordan and Payne, 1980; Payne and McNabb, 1984; deGouw et al., 2011).

Only six of the 62 floating oils studied herein were specifically analyzed for BTEX and selected volatiles (<n-C_{11}) using modified EPA Method 8260 (Douglas et al., 2015). Benzene was not detected in any floating oil samples although toluene (nd to 3.9 μg/g), ethylbenzene (nd to 0.80 μg/g), and total xylenes (nd to 5.9 μg/g) were (Table S-2). These concentrations are significantly lower than the fresh Macondo oil (2350 μg/g benzene, 6500 μg/g toluene, 1270 μg/g ethylbenzene, and 9010 μg/g total xylenes; Table S-2). The percent depletions of VOCs (in this case relative to n-C_{11}, rather than hopane; Eq. (1)) reveal some floating oils experienced higher depletions among BTEX and C_3- and C_4-alkylbenzenes relative to less soluble n-alkanes and other aliphatic VOCs (e.g., Fig. S-5A), which is consistent with preferential dissolution of the relatively soluble aromatics during the oil's ascent to the surface. In some floating oil dissolution was extensive resulting in 100% depletion of BTEX and C_3- and C_4-alkylbenzene while n-alkanes and other aliphatic VOCs were retained, reduced in a manner consistent with evaporation (e.g., Fig. S-5B). Finally, in other floating oils evaporation dominated the depletion of C_3- and C_4-alkylbenzenes and overprinted any loss of BTEX that may have occurred due to preferential dissolution (Fig. S-5C), with evaporation continuing in some floating oils to eventually remove all VOCs below n-C_{11} (Fig. S-5D).

The reduction of n-alkanes below n-C_{13} in the recently surfaced oil (Fig. 2B) appears consistent with loss due to dissolution and perhaps evaporation, with the latter starting to reduce these compounds within seconds of the sheens forming at the surface (Fig. S-3). Quantified n-alkanes between n-C_9 and n-C_{12} were decreasingly depleted with increasing carbon number between 88 and 5 wt% (Fig. S-6 A). As described in the previous paragraph (Fig. S-5), preferential losses of more soluble saturated (<C_7) and aromatic (BTEX and C_3-alkylated benzenes) compounds below n-C_{13} that occurred prior to or upon reaching the sea surface were quickly overprinted by the loss of volatile compounds due to evaporation after reaching the sea surface.

The GC-FID of the most weathered floating oil studied clearly shows a loss of compounds up to n-C_{23} (Fig. 2C). Based upon the HTSD results of the unweathered oil, this loss is estimated to be approximately 50 to 60 wt% of the oil. Percent depletion calculations (Eq. (1)), however, show 100% depletion of n-alkanes below n-C_{15} with depletions between n-C_{16} and n-C_{27} decreasing from 98 to 9 wt% (Fig. S-6B). The reduction of n-alkanes above n-C_{20} was common among the floating oils studied and is attributed to severe evaporation under the spill conditions, rather than biodegradation within the floating (coalesced) oils studied. Evidence that biodegradation is not responsible is found in the comparable percent depletions observed between n-alkane/isoprenoid pairs, i.e., n-C_{17}/pristane and n-C_{18}/phytane among even the most weathered floating oil (Fig. S-6B). As such, there is no significant change in n-C_{18}/Ph ratios between fresh Macondo oil and the floating oils (Fig. 2A–C). In addition, the floating oils also exhibited reductions among unresolved compounds resulting in a shift in the unresolved complex mixture (UCM) "hump" consistent with evaporation (Fig. 2C). Even though evaporative losses beyond n-C_{20} are rarely recognized in oil spills (Fingas, 1994; Prince et al., 2002), in this instance it is reasonable that the high air temperatures (28–30 °C) and high insolation in the northern GoM during the DWH spill allowed for severe evaporation in the floating oils.

The apparent lack of biodegradation of n-alkanes among the floating oils studied contrasts that observed in laboratory studies of Macondo oil (Bacosa et al., 2015). These researchers evaluated the effects of biodegradation and photo-oxidation on n-alkanes in chemically-dispersed and non-dispersed oils and showed that biodegradation dominated their removal and began within 5 to 10 days (faster in dispersed oil). The relatively rapid biodegradation of n-alkanes in floating oils observed in this laboratory study is likely explained by the low concentration of oil used (200 mg/L), compared to the coalesced slicks, mousses, and sheens sampled in the field during the DWH event. This is an important difference since biodegradation in coalesced (non-dispersed) floating oil must occur at the oil–water interface and in the presence of nutrients (e.g., nitrogen and phosphorous; Prince et al., 2013). The apparent lack of biodegradation in the coalesced floating oils studied herein was likely limited due to the relatively small mass of oil in contact with water and perhaps further retarded by the limited availability of nutrients in GoM surface water (Edwards et al., 2011).

The stranded Macondo oils also exhibited a range in weathering, although there was an overlapping among the least weathered stranded oils and the most weathered floating oils. The least weathered stranded oil found along the coastline exhibited a complete loss of compounds below n-C_{12} with at least some reductions extending up to about n-C_{22} (Fig. 2D). Based upon the HTSD results of the unweathered oil, this loss is estimated to be approximately 40 to 50 wt% of the oil. Quantified n-alkanes exhibited 100% depletion below n-C_{12} with depletions between n-C_{13} and n-C_{22} decreasing from 99% to 2% (Fig. S-6C). As with the floating oils this loss is attributable to evaporation (not biodegradation), since biodegradation of n-alkanes relative to isoprenoids was not evident in the n-C_{18}/Ph ratio (Fig. 2D).

As weathering progressed some of the most highly weathered stranded Macondo oils exhibited a complete loss of compounds below n-C_{16} with at least some reduction of n-alkanes above n-C_{20} (Fig. 2E). Quantified n-alkanes exhibited 100% depletion below n-C_{16} with depletions between n-C_{17} and n-C_{35} decreasing from 99% to 13% (Fig. S-6D). Although evaporation likely (initially) contributed to the depletion of n-alkanes, biodegradation of n-alkanes had clearly commenced in some of the most highly weathered stranded oils. This is evidenced by both the depletion of very long-chain n-alkanes (>n-C_{30}) that cannot reasonably be expected to evaporate, and in the higher percent depletions observed among n-alkanes (n-C_{17} and n-C_{18}) relative to isoprenoids (pristane and phytane; Fig. S-6D), the latter of which results in decreased n-C_{18}/Ph ratios (Fig. 2E). Thus, although biodegradation of n-alkanes was not observed among the coalesced floating oils studied, nor among most stranded oils studied, some of the most highly weathered stranded oils collected within seven weeks of the end of the DWH oil spill (e.g., Fig. 3E) had begun to biodegrade.

3.2. Polycyclic aromatic hydrocarbons

Table 3 contains the concentrations of PAHs and related compounds (e.g., decalins and sulfur-containing aromatics) measured in fresh Macondo oil and in the least and most weathered representatives of the floating and stranded oil populations studied. Included are the average PAH concentrations among the floating and stranded oils. The bottom of Table 3 contains two different total PAH concentrations, viz., (1) $TPAH_{50}$ refers to the sum of the 50 target analytes between naphthalene and benzo(*g*,*h*,*i*)perylene (excluding the "biogenic" PAHs, retene and perylene) and (2) $PetPAH_{27}$ refers to the sum of just 27 alkylated PAHs and dibenzothiophene homologs, which are more typical of

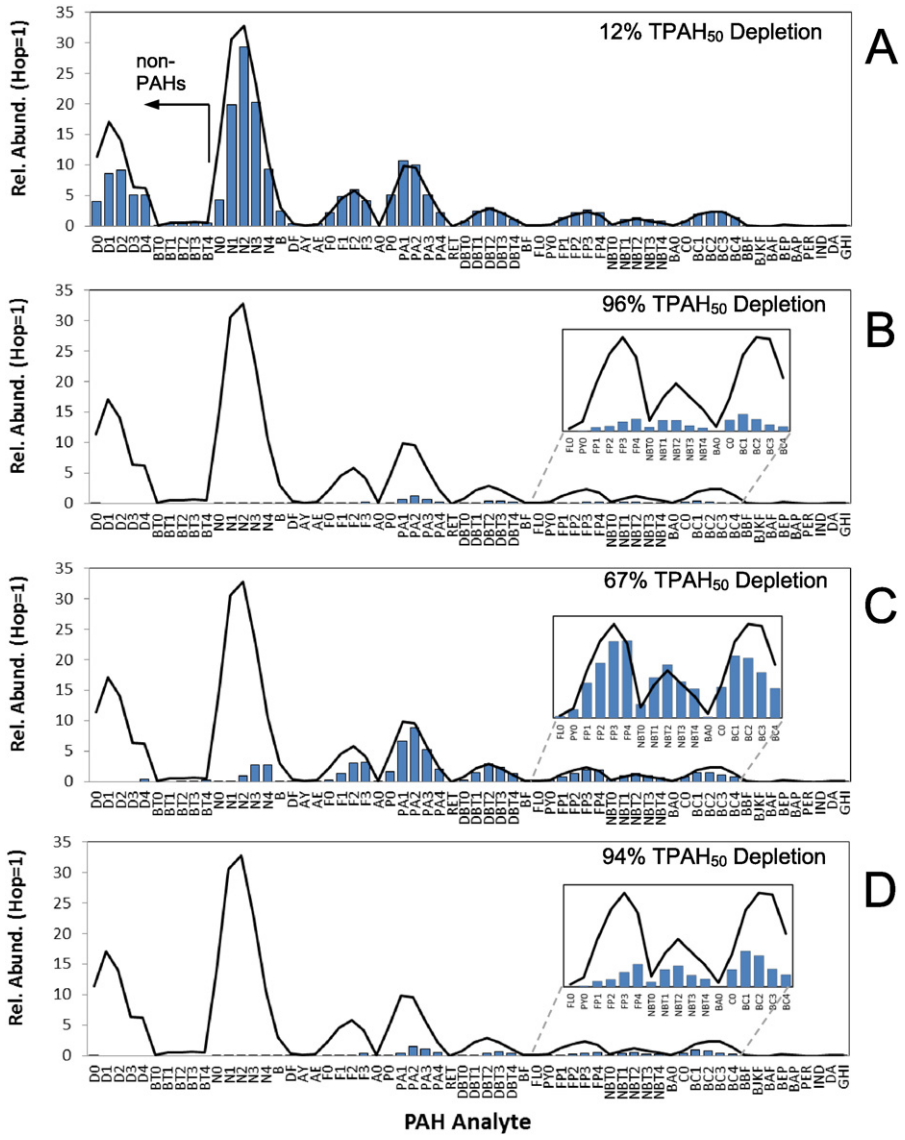

Fig. 3. Hopane-normalized histograms of decalins, PAHs, and sulfur-containing aromatics in representatives of the (A) least weathered floating oil, (B) most weathered floating oil, (C) least weathered stranded oil, and (D) most weathered stranded oil from 2010 compared to average fresh Macondo oil (black line). Compound abbreviations and absolute concentrations from Table 3. Insets show homolog patterns among fluoranthenes/pyrenes (FL0-FP4), naphthobenzothiophenes (NBT0-4) and benz(a)anthracenes/chrysenes (Ba0, C0, BC1–BC4). $TPAH_{50}$ refers to analytes between N0 and GHI, excluding Ret and Per.

petroleum. TPAH50 is discussed throughout the present paper, but $TPAH_{27}$ is included since it was useful for recognizing the impact of Macondo oil in nearshore sediments (in research to be published separately), wherein non-petroleum (pyrogenic) PAHs can occur and increase $TPAH_{50}$ concentrations irrespective of the presence/absence of Macondo oil. However in this study, $TPAH_{50}$ is emphasized since our focus is on oil weathering (not mixing with background PAH in sediments).

The $TPAH_{50}$ concentration in fresh Macondo oil (13,300 ± 507 μg/g) exceeds that of the average floating Macondo oils (6640 ± 4140 μg/g), which in turn exceeds the average of the stranded Macondo oils (1705 ± 746 μg/g; Table 3). This decreasing concentration trend represents an average depletion of $TPAH_{50}$ of 69 ± 23% in the floating oils and 94 ± 3.1% in the stranded oils studied. Thus, not surprisingly, weathering decreased the total concentration of PAH in floating and stranded Macondo oil. However, it's notable that the least weathered floating oil – as represented by the sample collected immediately after surfacing – contained a slightly higher $TPAH_{50}$ concentration (13,700 μg/g) than fresh Macondo oil (13,300 μg/g; Table 3). This initial increase in PAH concentration is due to the concentrating effects that dissolution (of soluble compounds during the oil's ascent to the surface) and possibly rapid evaporation (of volatile compounds upon reaching the surface) had on oil as it surfaced.

Fig. 3 shows the hopane-normalized histograms for PAHs and related compounds in the least and most weathered representatives of floating and stranded oils studied versus unweathered Macondo oil. (Corresponding percent depletions of individual PAH analytes for these four oils are shown in Figure S-7.) Inspection reveals that the least weathered floating Macondo oil collected immediately upon surfacing exhibits a PAH distribution very similar to unweathered Macondo oil (Fig. 3A). The 12% depletion in $TPAH_{50}$ in this sample is mostly expressed by the losses of C_0- to C_2-naphthalenes from the floating oil (N0–N2; Fig. 3A), which are 69 to 11% depleted (Fig. S-7A). The depletion of these 2-ring aromatics is mostly due to dissolution during the oil's ascent. Evidence for the dominant effect dissolution is shown in Fig. S-8 wherein naphthalene consistently exhibited a greater depletion than the less soluble, but comparably volatile n-C_{12} in all floating oils studied, particularly in the oil collected immediately upon surfacing. Decalins (D0-D4; decahydronaphthalenes) are also depleted, and given their relatively low aqueous solubility (compared to

naphthalenes), their depletion is most likely due to their rapid evaporation after reaching the surface although some dissolution during the oil's ascent is also possible. Despite the 12% depletion in $TPAH_{50}$, as noted above, the absolute concentration of $TPAH_{50}$ in the recently surfaced oil is slightly higher than in unweathered Macondo oil (Table 3), because hopane was also concentrated during dissolution weathering (removal) of the more water-soluble components below n-C_{10} that make up 25% by weight of the oil. This slight increase in $TPAH_{50}$ concentration is reflected by a balance between the dissolution losses of N0-N2 and slight excesses of C_{0-} to C_1- alkylated homologs of fluorenes (F), phenanthrenes/anthracenes (PA) and dibenzothiophenes (DBT; Fig. 3A).

The most weathered floating oil studied contains only 1090 μg/g $TPAH_{50}$, which represents a 96% depletion of $TPAH_{50}$ compared to the unweathered oil (i.e., much higher than average among floating oils; Table 3). All of the PAH homologs are markedly reduced in this highly weathered floating oil relative to unweathered oil (Fig. 3B) and also to the recently surfaced oil (Fig. 3A). C_0- to C_4-naphthalenes are 100% depleted and C_0- to C_3-fluorenes are 100% to 93% depleted causing C_0- to C_4-phenanthrenes, although 98 to 87% depleted themselves (Fig. S-7B), to become the dominant PAHs present in this sample (Fig. 3B). Variously alkylated fluoranthrenes/pyrenes are also significantly depleted (83–94%; Fig. S-7B) with the most highly alkylated homolog (FP4) becoming dominant (Fig. 3B inset). The relative retention of more highly alkylated homologs is consistent with typical PAH homolog weathering profiles observed elsewhere, which are attributed by the combined effects of evaporation, dissolution, and biodegradation (e.g., Elmendorf et al., 1994; Douglas et al., 1996). Notably however, a different profile is evident within the alkylated naphthobenzothiophene (NBT0-NBT4) and benz(a)anthracene/chrysene homologs (C0 to BC4) in which the C_1-homologs (NBT1 and BC1) are dominant and concentrations decrease at higher degrees of alkylation (Fig. 3B inset). These atypical homolog patterns are attributed the effects of photo-oxidation (Prince et al., 2003, Maki et al., 2001, Garrett et al., 1998), which is discussed further below.

Fig. 3C shows the hopane-normalized histogram for PAHs and related compounds in the least weathered stranded oils. The least weathered stranded Macondo oil studied had experienced a 67% depletion in $TPAH_{50}$ (Table 3) mostly attributable to the 100% depletion of C_0- and C_1-naphthalenes and 97 to 74% depletion of C_2- to C_4-naphthalenes (Fig. S-7C). The loss of the naphthalenes is attributed to the combined effects of evaporation and dissolution (Fig. 3C), both of which have clearly advanced the weathering relative to the recently surfaced oil (Fig. 3A). The difference between the recently surfaced oil (Fig. 3A) and the "freshest" oil to be found along shorelines (Fig. 3C) testifies to the loss of PAHs during the oil's transport to shorelines. Fluorene, phenanthrene, and dibenzothiophene homologs are also reduced with the greatest depletions being evident among the C_0- (non-alkylated) parents and decreasing depletion with increasing degree of alkylation (Figs. 3C and S-7C). These typical weathered homolog patterns are attributed to the combined effects of evaporation and dissolution. Although biodegradation could also produce such homolog patterns, it seems unlikely to be responsible here given that n-alkanes are not yet biodegraded in this (and most other) stranded oils (e.g., Fig. 2C; see discussion above). Close inspection of the naphthobenzothiophene and benz(a)anthracene/chrysene homologs reveals that the former are not depleted while the latter are slightly depleted and exhibit the atypical homolog pattern consistent with photo-oxidation (see Fig. 3C inset, and discussion below). The fact that the naphthobenzothiophenes are not yet affected by photo-oxidation, while the benz(a)anthracenes/chrysenes are, indicates the former appear (at least initially) less susceptible to photo-oxidation. This disparity is consistent with Andersson (1993), who found that the sulfur-containing aromatics are generally less susceptible to photo-oxidation than PAHs.

The hopane-normalized histogram for the representative of the most weathered stranded oil is shown in Fig. 3D. This sample exhibits a 94% depletion of $TPAH_{50}$ (Table 3), which is the same magnitude depletion exhibited by the average among all 1174 stranded oils studied (Table 3). This indicates that most of the 1174 stranded oils studied were comparably weathered to the most weathered representative shown in Fig. 3D). C_0- to C_4-naphthalenes were 100% depleted and C_0- to C_3-fluorenes were 100% to 92% depleted from most stranded oils causing C_0- to C_4-phenanthrenes, although 100 to 76% depleted themselves (Fig. S-7D), to become the dominant PAHs remaining (Fig. 3D). C_0- to C_4-dibenzothiophenes and fluoranthene/pyrene homologs are also depleted (100 to 64% and 94 to 70%, respectively) with the more highly alkylated homologs in each being the least depleted (Fig. S-7D). As noted above, this homolog pattern is consistent with the combined effects of dissolution and evaporation, although among stranded oil biodegradation may have also contributed (since biodegradation had commenced in the most highly weathered stranded oils; see Fig. 2E and discussion above). However, also as noted above, an atypical homolog profile is evident within the naphthobenzothiophene and benz(a)anthracene/chrysene in the most weathered stranded oil (Fig. 3D inset). This atypical pattern is consistent with the effects of photo-oxidation as discussed in the following paragraphs.

While the least and most weathered representatives reveal the range in weathering of PAHs in floating and stranded Macondo oils during and shortly following the DWH oil spill (Figs. 3 and S-7), the average percent depletion of individual PAH analytes in these two populations clearly reveals the overall progression in and different processes responsible for the weathering (Fig. 4).

On average, the depletions among decalin, benzothiophene, dibenzothiophene, and all 2- and 3-ring PAH homologs in the floating and stranded Macondo oils exhibited a typical pattern of PAH weathering in which the percent depletions decreases with increasing degree of alkylation (see downward pointing arrows in Fig. 4). In addition, the absolute amounts of these depletions tend to decrease with increasing ring number so that, for example, the depletions among 2-ring naphthalenes (98 to 66%) exceed those of 4-ring fluoranthrenes/pyrenes (43 to 29%) with losses among 3-ring phenanthrenes/anthracenes and dibenzothiophenes being intermediate and mostly equal. These typical homolog depletion patterns are attributable to the combined effects of evaporation and dissolution, which would promote the loss of compounds with higher vapor pressures and higher aqueous solubilities. The stranded oils (Fig. 4B), on average, consistently exhibit higher percent depletions than the floating oils (Fig. 4A), testifying to the progression in evaporation and dissolution, and perhaps in some of the more highly weathered stranded oils also biodegradation, during the oil's transport to and/or weathering after reaching the shore.

Depletions among naphthobenzothiophene and benzo(a)anthracenes/chrysene homologs in the floating and stranded oils exhibit an atypical pattern of PAH weathering in which the percent depletions increase within increasing degree of alkylation (see upward pointing arrows in Fig. 4). This atypical pattern is consistent with photo-oxidized oils (Garrett et al., 1998; Maki et al., 2001; Prince et al., 2003; King et al., 2014; Radović et al., 2014) in which the greater depletion among more highly alkylated homologs is observed. This effect is also enhanced by the molecular weight of the PAH, so that chrysenes are relatively more depleted than phenanthrenes (Garrett et al., 1998; Lee, 2003). The greater depletion of more highly alkylated naphthobenzothiophenes and benz(a)anthracenes/chrysenes in the floating and stranded Macondo oils (Fig. 4) indicates they suffered significant losses due to exposure to uv radiation. Notably, the depletions among benz(a)anthracenes/chrysenes exceeds those among naphthobenzothiophenes in both the floating (Fig. 4A) and stranded (Fig. 4B) oils indicating the sulfur-containing naphthobenzothiophenes appear less sensitive to photo-oxidation than the hydrocarbons (as previously observed; Andersson, 1993).

The observation that photo-oxidation has affected the floating and stranded oils studied is notable since such transformations are considered ~100-times less efficient in oil (compared to dissolved PAH in

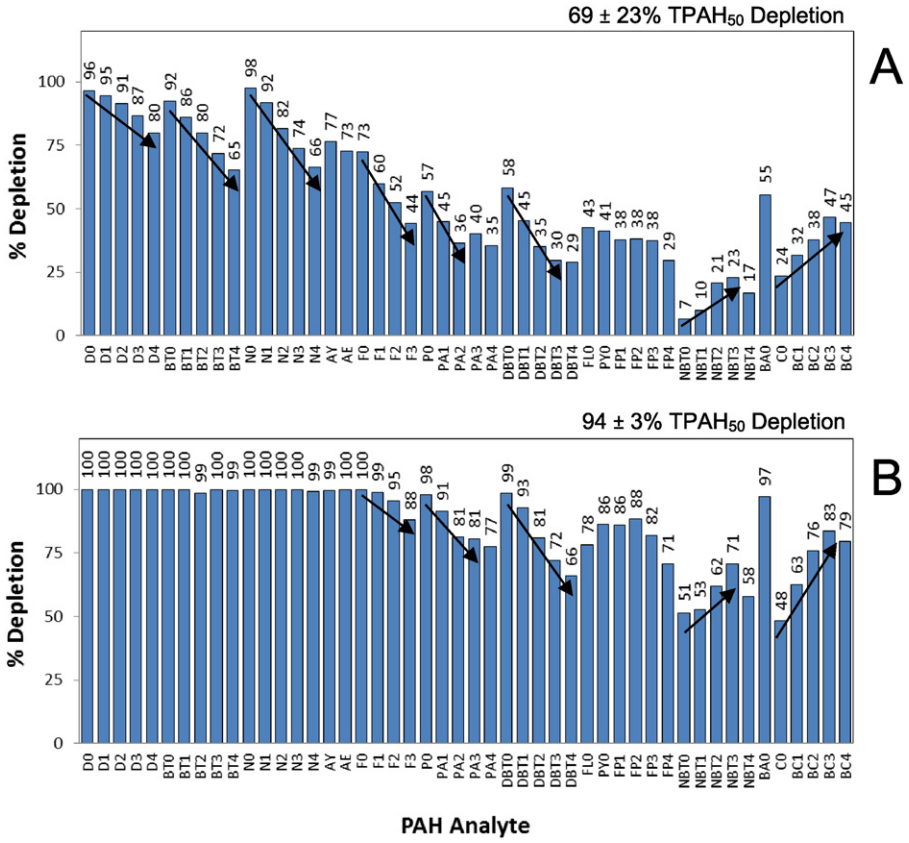

Fig. 4. Average percent depletions of individual PAHs and homolog groups in the populations of (A) floating Macondo oils (n = 62) and (B) stranded Macondo oils (n = 1174) from 2010. %depletions relative to hopane calculated as per (1). Compound abbreviations from Table 3. Arrows indicate trends within homolog groups.

water) due to the attenuating properties of the hydrophobic oil (Plata et al., 2008). Clearly, the high insolation that existed in the northern GoM quickly promoted enhanced and rapid photo-oxidation of the Macondo oil that had reached the sea surface and traveled to shorelines during the 87-day spill and in the following months. As reported elsewhere (Aeppli et al., 2012), oxidized hydrocarbons (in part formed via photo-oxidation) comprised more than 50% of the mass of stranded Macondo oils collected in 2011 (later than the stranded oils studied herein). This is an important observation, viz., depletion of target PAHs (Fig. 4) does not mean the mass of the oil is proportionately decreasing due to photo-oxidation, but that these PAHs are being converted into oxidized derivatives of PAHs.

Finally, the floating and stranded oils exhibit no clear trend in the levels of depletion among the C_0- to C_4-fluoranthrene/pyrene homologs (Fig. 4), perhaps testifying to the competing effects of evaporation and dissolution versus photo-oxidation on these PAHs.

Additional evidence of photo-oxidation is seen in the different effects among individual PAH isomers. For example, it is evident that benz(a)anthracene (BA0) exhibited approximately twice the degree of depletion than its isomer chrysene (C0) in both floating and stranded oils (Fig. 4). This difference likely results from benz(a)anthracene's greater susceptibility to photochemical degradation (Plata et al., 2008). In addition, inspection of individual methyl-fluoranthene/pyrene and methyl-chrysene isomer patterns reveals isomer-specific changes also attributable to photo-oxidation of specific isomers previously recognized as being relatively susceptible to photo-oxidation (Fig. 5). The floating oil sampled immediately upon surfacing shows no change in isomer pattern from the fresh oil. However, the severely weathered floating oil demonstrates a preferential depletion of the 1-methylpyrene (1MPy) as well as all three benzofluorene isomers (BaF, BbF, and BcF) relative to the 4- and 2-methylpyrene (4MPy and 2MPy) in the *m/z* 216 extracted ion profile (EIP). Preferential photo-oxidation of 2-, 6- and 1-methylchrysene isomers was also observed relative to 3-methylchrysene in the *m/z* 242 EIP (Fig. 5).

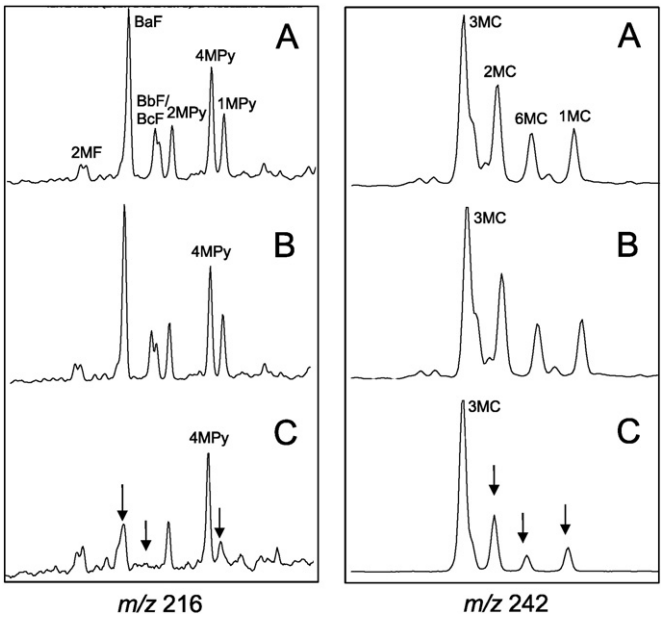

Fig. 5. Partial EIPs showing methyl-fluoranthrenes/pyrenes and benzofluorenes (*m/z* 216; left) and methyl-chrysenes (*m/z* 242; right) isomer patterns in (A) fresh Macondo oil, (B) minimally-weathered floating oil collected immediately upon surfacing (JF3-2 km-onet-20100616-surf-N143) and (C) a severely-weathered floating Macondo oil (GU-10-02005-T-003). Isomer specific reductions in (C; arrows) are attributed to photo-oxidation.

3.3. Spatial and temporal weathered trends

The depletion of $TPAH_{50}$ in the floating and stranded oils studied provides insight to the spatial and temporal changes to the oil during and shortly following the spill. Fig. 6 shows the percent depletion of $TPAH_{50}$ in the oils versus their distance from the well, and the inset table shows the average $TPAH_{50}$ depletions for samples collected at different distances and times during and shortly following the DWH oil spill. At the most basic level Fig. 6 reveals that the "freshest" floating oils were found closest to the well and the "freshest" stranded oils were found on the closest shoreline(s) about 75 to 80 km away (i.e., the Mississippi River birdfoot; Fig. 1). Additional details are revealed upon closer inspection of these data.

Floating oil samples collected less than 10 km from the wellhead exhibited a wide range of $TPAH_{50}$ depletion (12 to 91%), which averaged 54 ± 20%. This wide range among floating oils close to the well is not surprising since "fresh(er)", newly released oil was continually reaching the surface every day (such as the recently surfaced oil studied herein; Fig. 3A). The PAHs in these oils were rapidly reduced by evaporation imparting the wide range observed within relatively short distances from the well. The continual re-supply of oil nearest the well is reflected in the consistent average levels of $TPAH_{50}$ depletion for floating oil samples within 10 km of the well in both May (54 ± 15%) and June (53 ± 35%), i.e., during the active spill.

The wide range observed within 10 km of the well quickly decreases for floating oils collected 10 to 75 km from the well that, on average, exhibited 85 ± 14% depletion of $TPAH_{50}$. This indicates that weathering of the floating oil quickly advanced as the oil moved away from the well. Based upon the results above (Figs. 3 and 4) it appears weathering was due to a combination of evaporation and photo-oxidation. There was no change in the $TPAH_{50}$ depletion among floating oils collected 10 to 75 km from the well in May, June, or July, indicating the continual re-supply of "fresh(er)" oil near the well in turn replenished the floating oils found further from the well. Thus, among the floating oils the distance from the well had a greater effect on the degree of $TPAH_{50}$ depletion than the collection date.

Stranded oil samples also exhibited a progressive increase in $TPAH_{50}$ depletion with increasing distance from the well (Fig. 6). On average, the $TPAH_{50}$ depletion increased from 89 ± 8% to 95 ± 3% between 75 and 350 km from the well (Fig. 6 inset). However, unlike the floating oils, there is evidence that a temporal trend is superimposed upon this spatial trend for stranded oils. Specifically, the "freshest" stranded oils (68 ± 1% $TPAH_{50}$ depletion) were collected in May 2010 relatively close to the well (75–125 km) within the Mississippi River birdfoot area (Fig. 1). Samples collected at this same distance/area in June and July were much more depleted (90 ± 5% and 92 ± 4%, respectively). Stranded oils collected 125 to 200 km from the well also exhibit a smaller but still measurable increase in $TPAH_{50}$ depletion for samples collected in May (89 ± 2%), June (92 ± 3%), July (94 ± 2%), August (94 ± 3%), and September (95 ± 3%; Fig. 6 inset). Although exceptions certainly exist, on average, this suggests that the degree of weathering among stranded oils generally increased with both distance from the well and the passage of time.

3.4. Effect of weathering on PAH-based source ratios

Based upon the Results and discussion above it is evident that ratios between PAHs that are often used in oil spill source identification are subject to change due to the extensive depletion among most PAH analytes (Fig. 4). Of particular relevance are the ratios of alkylated dibenzothiophenes to alkylated phenanthrenes, which have been long used as source ratios owing to the variable amounts of sulfur in petroleum from different sources (Douglas et al., 1996). Specifically, the ratios of C_2- and C_3-dibenzothiophenes to C_2- and C_3-phenanthrenes (DBT2/PA2 and DBT2/PA3) vary among different oils and reportedly remain stable during laboratory biodegradation studies in which 98% of the total PAHs were removed (relative to hopane; Douglas et al., 1996).

Fig. 7 shows the DBT2/PA2 and DBT3/PA3 ratios for the 62 floating and 1174 stranded Macondo oils studied versus the percent depletion for the numerator in each ratio (per Eq. (1)). The DBT2/PA2 ratio remains stable during weathering until approximately 60% of the DBT2 is depleted, after which there is considerable scatter until the DBT2/PA2 ratio increases at DBT2 depletions above 90% (Fig. 7A). This indicates that the C_2-dibenzothiophenes and the C_2-phenanthrenes are being weathered at comparable rates up to about 60% depletion of DBT2. As weathering exceeds this level, however, considerable scatter is introduced to the DBT2/PA2 ratio. The DBT3/PA3 ratio immediately increases as DBT3 is depleted indicating that C_3-phenanthrenes are being depleted preferentially over the C_3-dibenzothiophenes (Fig. 7B). This disparity is evident in the average percent depletions for DBT3 and PA3 in both the floating (30% and 40%, respectively; Fig. 4A) and stranded oils (72% and 81%, respectively; Fig. 4B).

No such disparity was observed in the laboratory biodegradation studies of Douglas et al. (1996), however, these researchers did not include any effect of photo-oxidation in their experiment. We attribute this disparity to preferential photo-oxidation of the C_3-phenanthrenes

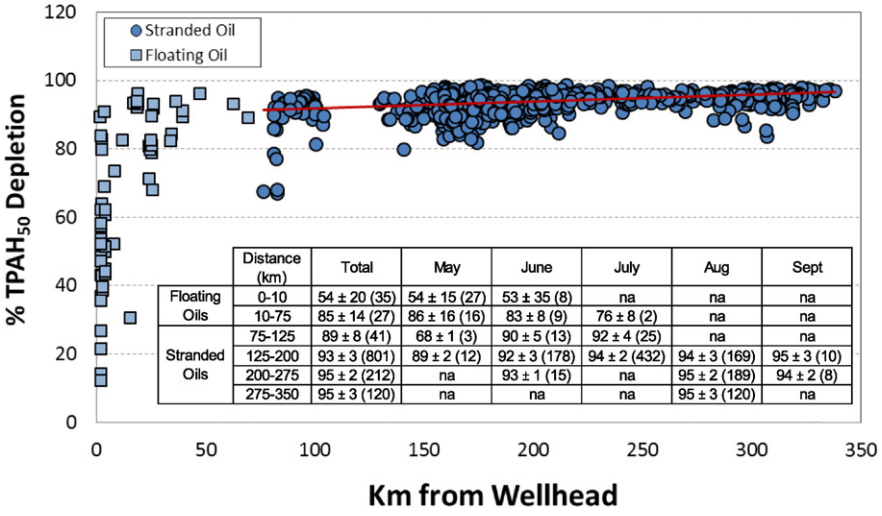

	Distance (km)	Total	May	June	July	Aug	Sept
Floating Oils	0-10	54 ± 20 (35)	54 ± 15 (27)	53 ± 35 (8)	na	na	na
	10-75	85 ± 14 (27)	86 ± 16 (16)	83 ± 8 (9)	76 ± 8 (2)	na	na
Stranded Oils	75-125	89 ± 8 (41)	68 ± 1 (3)	90 ± 5 (13)	92 ± 4 (25)	na	na
	125-200	93 ± 3 (801)	89 ± 2 (12)	92 ± 3 (178)	94 ± 2 (432)	94 ± 3 (169)	95 ± 3 (10)
	200-275	95 ± 2 (212)	na	93 ± 1 (15)	na	95 ± 2 (189)	94 ± 2 (8)
	275-350	95 ± 3 (120)	na	na	na	95 ± 3 (120)	na

Fig. 6. Weathering ($TPAH_{50}$ depletion) in floating (n = 62) and stranded (n = 1174) Macondo oils collected during and within six weeks of the DWH oil spill versus distance from the Macondo well (km). Inset table shows $TPAH_{50}$ depletion Avg. ± 1σ (n) for different sample collection periods. na: no samples collected. Line depicts linear best fit for all stranded oils; $\%TPAH_{50}$ depletion = 0.02 × km + 90.

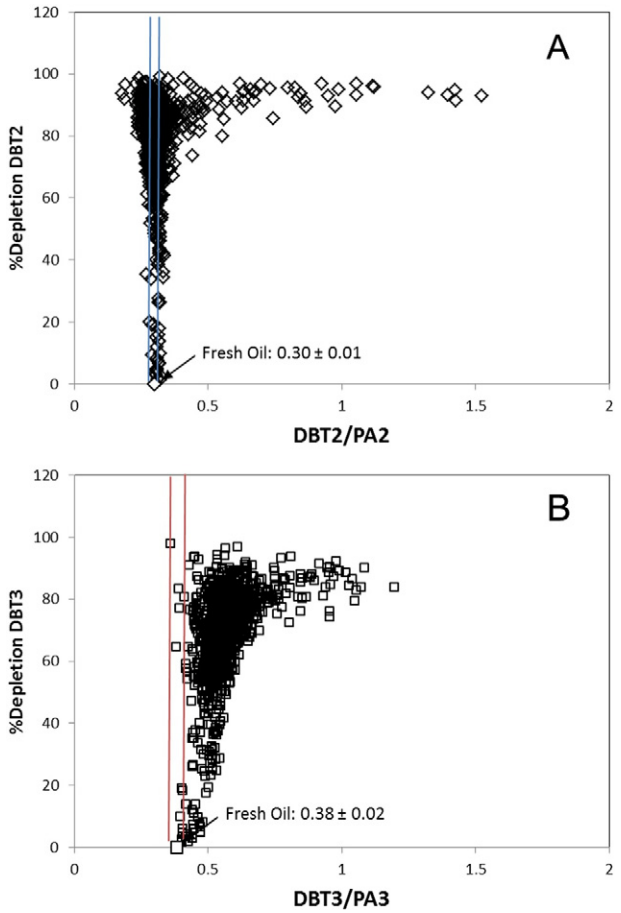

Fig. 7. Trends in the common source ratios (A) DBT2/PA2 and (B) DBT3/PA3 versus percent depletion of the alkylated dibenzothiophenes for the floating and stranded Macondo oils studied. Average ± 1 standard deviation for fresh Macondo oil is indicated.

over C_3-dibenzothiophenes in the naturally-weathered floating and stranded Macondo oils studied herein (which is consistent with earlier laboratory studies showing lower susceptibility among sulfur-containing aromatics; Andersson, 1993). The effects of weathering, particularly photo-oxidation, on these common PAH-based sourced ratios warrant caution in using these ratios to "fingerprint" weathered Macondo oils in the GoM coastal environments. In addition, dissolution enhanced by the application of dispersant may similarly affect these ratios as observed in oil droplets isolated from water samples collected at depth where chemical dispersant was associated with the oil phase (Payne and Driskell, 2015b). Thus, the use of these "conventional" PAH-based source ratios must consider these weathering effects.

3.5. Biomarkers

The stability of biomarkers during weathering of spilled oil is a fundamental basis for their use in chemical fingerprinting (Wang et al., 2006). The floating and stranded Macondo oils studied herein exhibited highly stable terpane and sterane biomarker distributions regardless of the degree of weathering, which (along with GC-FID analysis) were used to confirmed the 62 floating and 1174 stranded oils studied were in fact Macondo oil. The floating and stranded oils, however, exhibited marked depletions in the relative and absolute concentrations of triaromatic steroid (TAS) biomarkers. These properties can be visualized in Fig. 8, which shows the hopane-normalized abundances of targeted (tricyclic and pentacyclic tri-) terpanes, (dia- and regular) steranes, and TAS in the least and most weathered representatives of the floating oils. (Absolute concentrations of biomarkers, compound abbreviations, along with the calculated depletions of total TAS, are given in Table S-3. Total TAS is defined as the sum of the four targeted congeners.)

The distributions and abundances of the individual terpanes (T4 to T35), steranes (S4 to S27), and the four TAS congeners in the least weathered floating oil, which was collected immediately upon surfacing (Table 1), are consistent with the unweathered Macondo oil (Fig. 8A). The TAS are not depleted (−2%) indicating these aromatic biomarkers, as well as the triterpanes and steranes were retained unaltered (and enriched per grams of oil due to loss of lower-molecular-weight soluble constituents; Table S-3) during the oil's ascent to the sea surface. However, the most weathered floating oil exhibits a 65% depletion in TAS, while the triterpanes and steranes remained unchanged (Fig. 8B). (A reduction in 14α(H),17α(H)-20S-ethylcholestane (S25) is evident, which is discussed further below.) The four individual TAS congeners exhibit percent depletions that narrowly range from 63 to 67% relative to hopane (Eq. (1)), which indicates the process(es) responsible for their depletion affected all four congeners similarly.

The depletion of the various TAS congeners was also observed by other researchers, who attributed their reduction in spilled and laboratory irradiated oils exclusively to photo-oxidation (Aeppli et al., 2014; Radović et al., 2014). The photo-reactivity of the TAS congeners is not surprising given their highly alkylated, 3-ring PAH structures, which are known to be particularly photo-sensitive (Garrett et al., 1998; Prince et al., 2003). It is notable that the most weathered floating oil studied (Fig. 8B) exhibits a greater depletion of TAS than the stranded oils (Fig. 8C–D; Table S-2), which argues that most oils reaching the shore had experienced less weathering than the most highly weathered floating oils studied herein. This same observation can be made with respect to the weathering of PAHs (Fig. 3).

3.6. Weathering plots

The weathering of PAHs and TAS described in the previous sections can be quantitatively illustrated using percentage weathering plots (PW-plots), such as are employed within the CEN (2012) oil spill identification protocol. PW-plots can be made by plotting the percent depletions (or retention) of individual analytes, in this case PAHs and biomarkers, relative to hopane (Eq. (1)) versus each analyte's relative retention times (RRT) from gas chromatographic analysis. RRTs are largely reflective of each compound's intrinsic properties, e.g., vapor pressure and solubility, which generally decrease with RRT among related compound groups. Thus, for PAHs a lower RRT generally reflects the greater susceptibility to evaporation. Weathering due to dissolution, biodegradation or photo-oxidation is revealed by deviations from trends attributable to evaporation.

Fig. 9 shows the PW-plots for the averages for the floating and stranded Macondo oil populations studied herein. The floating oils exhibit, on average, depletions of earlier eluting PAHs and related compounds (e.g., decalins and benzothiophenes) that decrease with increasing RRT, a trend which is consistent with losses due predominantly to evaporation (Fig. 9A). Close inspection reveals that naphthalene (N0) and C_1-naphthalenes (N1) exhibit ~5% higher depletions than decalins and benzothiophenes with comparable RRTs (Fig. 9A). This indicates that, while most naphthalene and methyl-naphthalenes were lost to evaporation, on average, an additional 5% was likely lost via dissolution of these relatively soluble 2-ring aromatics either during the oil's ascent or while at the sea surface. The stranded oils, on average, exhibit depletions among PAHs with RRT up to about 1800 that appear consistent with evaporation (Fig. 9B). Any losses of the more soluble PAHs due to dissolution appear to be masked by the effects of evaporation.

Evidence for photo-oxidation is clearly evident in both the floating and stranded oils, being more severe in the later. Specifically, later-eluting PAHs exhibit much higher depletions than steranes and hopanes, the latter of which are largely unaffected by weathering.

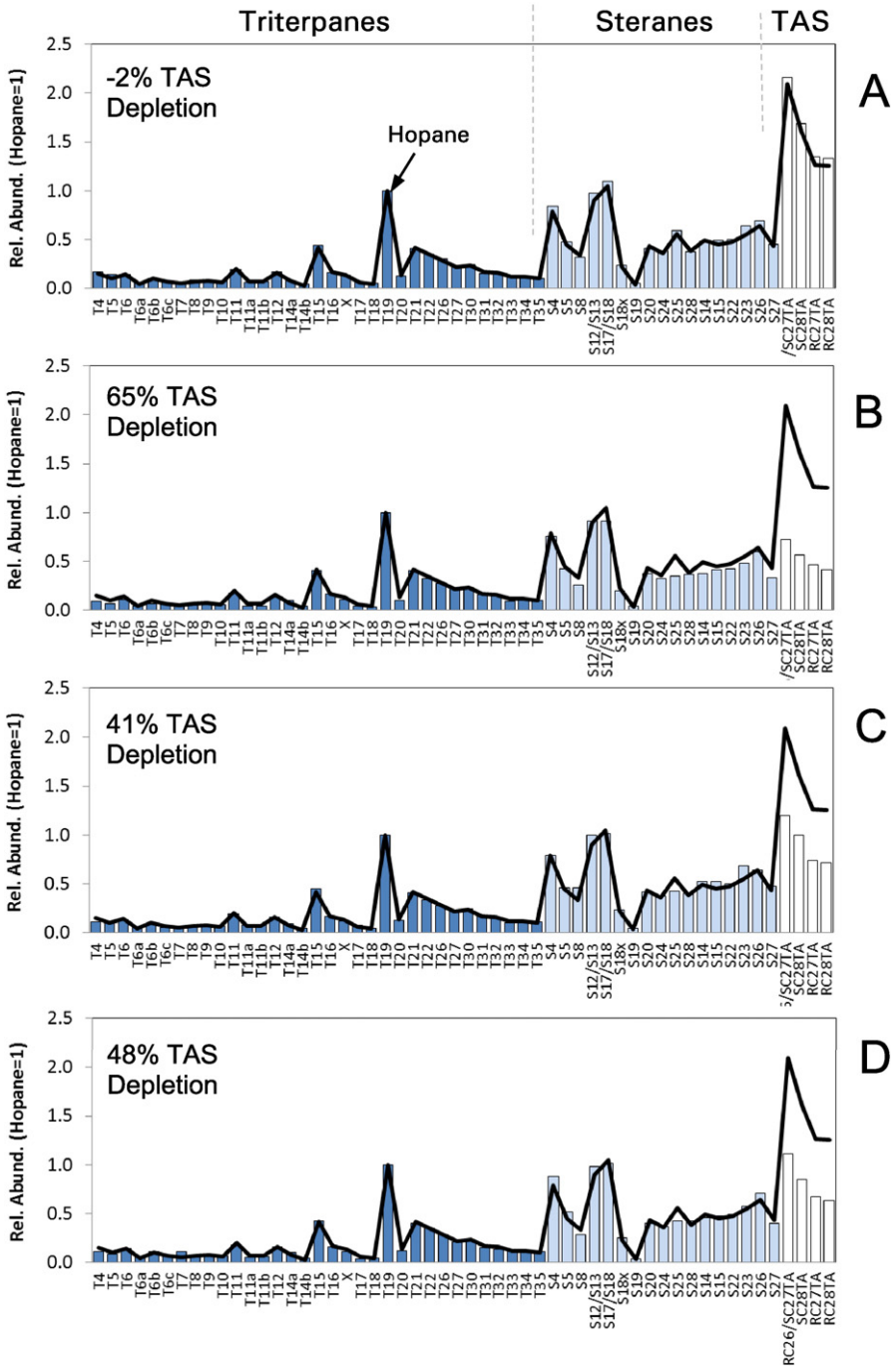

Fig. 8. Hopane-normalized histograms of biomarkers in representatives of the (A) least weathered floating oil, (B) most weathered floating oil, (C) least weathered stranded oil, and (D) most weathered stranded oil from 2010 compared to average fresh Macondo oil (black line). Compound abbreviations and absolute concentrations from Table S-3. Total triaromatic steroids (TAS) depletions relative to hopane ((1)) are given.

[Contrary to what was reported by Aeppli et al. (2014) we observed no depletion among C_{32}- to C_{35}-homohopanes in floating or stranded oils.] Photo-oxidation has preferentially depleted the more highly alkylated benz(a)anthracenes/chrysenes (BC2-BC4), fluoranthenes/pyrenes (FP2-FP4), and naphthobenzothiophenes (NBT2-NBT4), which plot well below the biomarkers with comparable RRTs (Fig. 9). The marked photo-oxidation of benz(a)anthracene (over chrysene) and the triaromatic steroids are also obvious, with both being more highly depleted in the stranded oil population. Notably, the alkylated naphthobenzothiophenes experienced slightly less depletion than the alkylated benz(a)anthracenes/chrysenes, owing to the former's lower susceptibility to photo-oxidation due to the presence of sulfur. This same disparity is evident in the comparison of alkylated dibenzothiophenes (DBT2 and DBT3) versus alkylated phenanthrenes (PA2 and PA3; Fig. 9), which is consistent with the increased DBT/PA ratios described above (Fig. 7). Finally, the depletion of 14α(H),17α(H)-20S-ethylcholestane (S25) compared to other biomarkers (Fig. 9) was unexpected but was noted above (Fig. 8B–D) and evident throughout our dataset. We attribute the apparent depletion in S25 to an analytical artifact of its co-elution among C_4-benz(a)anthracene/chrysene isomers (which becomes evident on the PW-plots), wherein there is a contribution to the S25 peak area in the *m/z* 217 extracted ion profiles by ions

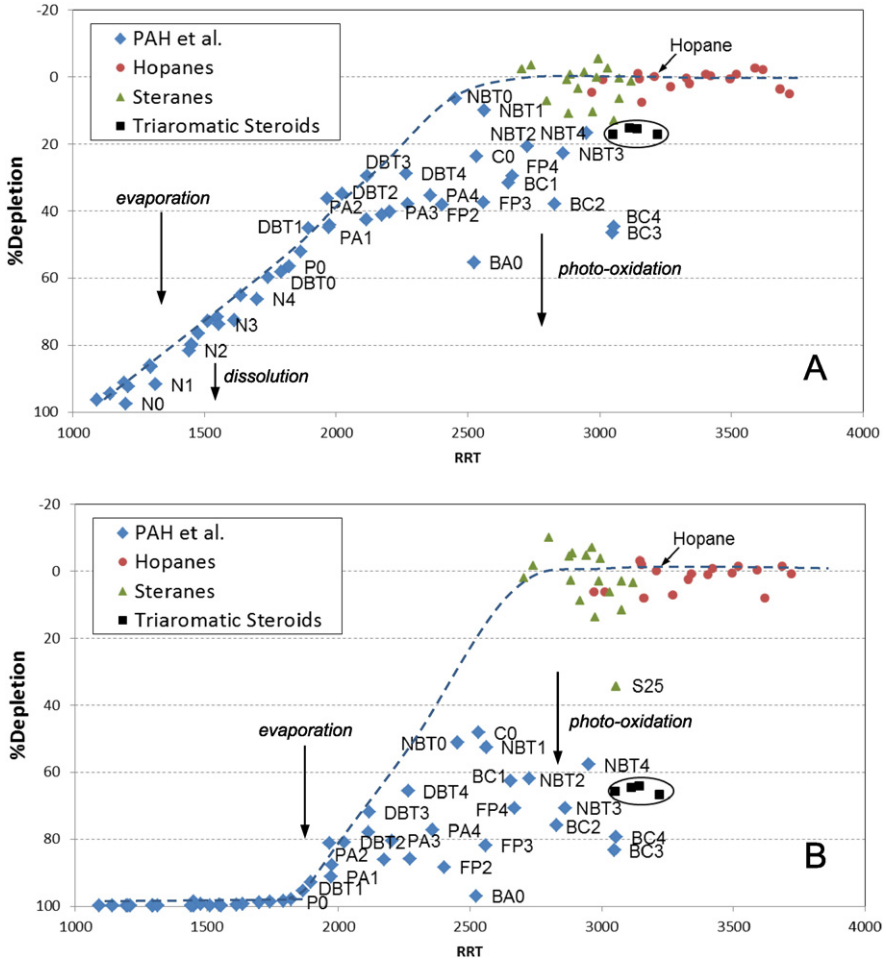

Fig. 9. Percent weathering plots for (A) average of floating Macondo oils (n = 62) and (B) average of stranded Macondo oils (n = 1174) from 2010. Selected PAH analyte labels from Table 3. Calculated from data in Table S-3. RRT refers to relative retention time of each analyte based on *n*-alkanes, viz., *n*-C_{10} = 1000, *n*-C_{20} = 2000, etc.

from the co-eluting C_4-benz(a)anthracenes/chrysenes. As these interfering C_4-benz(a)anthracenes/chrysenes are photo-oxidized S25 appears to be depleted.

4. Conclusions

The large populations of field-collected floating and stranded oils collected mostly during, but all within seven weeks of the DWH oil spill capture the full range of weathering experienced by the surfaced Macondo oil. Oil collected immediately after appearing at the sea surface had already lost most mass below *n*-C_8, with at least some reduction of all compounds below *n*-C_{13}; total mass loss is estimated at 20–25 wt%. Most mass loss is consistent with dissolution of more soluble aliphatics (<*n*-C_7), monoaromatics, and naphthalene and methylnaphthalene during the oil's ascent, although rapid evaporation may have also contributed during the brief time between when the rainbow-colored sheen formed at the surface and was sampled.

Some floating oil samples contained trace concentrations of toluene and C_2- to C_4-alkylbenzenes, although benzene was not detected. Higher percent depletions of these monoaromatics versus less soluble but comparably volatile aliphatics indicated preferential dissolution of the monoaromatics occurred during the oil's ascent or while at the surface. Evaporation eventually removed all volatiles below *n*-C_{11} in floating oils.

Weathering progressively altered the floating Macondo oils found offshore, with the most highly weathered floating oil exhibiting loss of mass below *n*-C_{15}, with at least some reductions extending up to *n*-C_{27}; total mass loss is estimated at 50–60 wt%. The reduction of *n*-alkanes above *n*-C_{20} was common among the floating oils studied and consistent with severe evaporation (decreasing depletion with increasing carbon numbers), but inconsistent with biodegradation (no change in *n*-C_{18}/Ph ratios) which had not yet commenced within the coalesced floating oils studied.

Stranded oils collected from shorelines during and shortly after the DWH spill were generally more highly and uniformly weathered than floating oils. The least weathered stranded oil exhibited a complete loss of compounds below *n*-C_{12} with at least some reductions extending up to about *n*-C_{22} due to evaporation; total mass loss is estimated at 40–50 wt%. The most weathered stranded oil exhibited a complete loss of compounds below *n*-C_{16} with at least some reduction of *n*-alkanes up to *n*-C_{35}; total mass loss is estimated at 70–80 wt%. Biodegradation had clearly begun to affect some stranded oils collected within seven weeks of the DWH spill (as evidenced by decreases in *n*-C_{18}/Ph ratios).

The PAHs in the floating and stranded oils showed dramatic changes due to weathering. The $TPAH_{50}$ concentration in fresh Macondo oil (13,300 ± 507 μg/g) exceeded that of the average floating Macondo oils (6640 ± 4140 μg/g) and stranded Macondo oils (1705 ± 746 μg/g), which represent average $TPAH_{50}$ depletions of 69 ± 23 and 94 ± 3.1%, respectively (relative to hopane). Despite a 12% depletion in $TPAH_{50}$ (due mostly to a 69% depletion of naphthalene) attributable to dissolution during the oil's ascent, oil collected immediately upon surfacing contained a slightly higher $TPAH_{50}$ concentration (13,700 μg/g) than fresh Macondo oil due to the concentrating effects of dissolution and evaporation (of more soluble and volatile compounds). The most weathered floating oil contained only 1090 μg/g $TPAH_{50}$ representing

a 96% depletion from the fresh oil. The least and most weathered stranded oils contained 8250 and 1540 μg/g $TPAH_{50}$ representing 67% and 94% depletions from the fresh oil, respectively.

Increased depletion of PAHs in the floating and stranded oils is attributed to the combined effects of evaporation, dissolution, and photo-oxidation; biodegradation of PAHs was unlikely given *n*-alkanes were not yet being biodegraded in any floating oils and most stranded oil samples. The combined effects of dissolution and evaporation removed naphthalenes, fluorenes, and phenanthrenes in floating and stranded oils, depleting the more highly alkylated homologs to lesser degrees. On the other hand, photo-oxidation preferentially depleted the more highly alkylated naphthobenzothiophene and benz(a)anthracene/chrysene homologs with the sulfur-containing naphthobenzothiophenes appearing (at least initially) less sensitive to photo-oxidation than benz(a)anthracenes/chrysenes. Fluoranthenes/pyrenes appear to have been intermediately depleted by the combined effects of dissolution, evaporation, and photo-oxidation. Susceptibility to photo-oxidation also varied among individual PAH isomers, e.g., preferentially affecting benz(a)anthracene over chrysene and specific C_1-fluoranthene/pyrene and chrysene isomers.

Not surprisingly the "freshest" floating oils were found closest to the well and the "freshest" stranded oils were found on the closest shoreline(s) about 75 to 80 km away (i.e., the Mississippi River birdfoot). Weathering generally increased among floating oils with increasing distance from the well, with oils less and more than 10 km exhibiting 54 ± 20 and 85 ± 14% depletions of $TPAH_{50}$, respectively, regardless of when the samples were collected owing to the continual resupply of "fresh(er)" oil near the well throughout the 87-day active spill period. Stranded oil samples also exhibited a smaller yet progressive increase in $TPAH_{50}$ depletion with distance from the well, increasing from 89 ± 8% to 95 ± 3% between 75 and 350 km from the well. On average, the percent depletions of $TPAH_{50}$ increased monthly during or within 7 weeks of the end of the spill indicating that weathering of stranded oils generally increased with both distance from the well and the passage of time.

The marked depletions among alkylated dibenzothiophenes and phenanthrenes increased commonly-used source ratios (DBT2/PA2 and DBT3/PA3) thereby warranting caution in using these ratios to "fingerprint" weathered Macondo oil in the GoM coastal environments. Petroleum biomarkers appear more stable and thereby reliable for use in fingerprinting surfaced Macondo oils. The stability of (tricyclic and pentacyclic tri-) terpanes and (dia- and regular) steranes was evident among all of the floating and stranded oils studied, regardless of the degree of weathering. However, total triaromatic steroids (TAS) are depleted in all of the floating (avg: 18 ± 26%) and stranded (avg: 65 ± 10%) oils studied except in the oil sampled immediately after surfacing. This result supports previous laboratory and field studies demonstrating the susceptibility of these polycyclic aromatic TAS biomarkers to photo-oxidation.

The overall extent and rapidity at which surfaced Macondo oil was weathered likely owe to the favorable conditions for weathering that existed during the DWH oil spill, viz., high surface water and air temperatures, high insolation, and (at least among stranded oils) indigenous microbes capable of degrading coalesced oil.

Disclosure

This study was conducted within the Deepwater Horizon NRDA investigation, which was cooperatively conducted by NOAA, other Federal and State Trustees, and BP. The scientific results and conclusion of this publication, as well as any views or opinions expressed herein, are those of the authors only. The authors declare no competing financial interest in the publication of this study. Funding for the study was provided by NOAA through Industrial Economics, Corp. (Cambridge, MA) as part of the NRDA process.

Acknowledgments

The authors wish to thank the efforts of numerous NRDA field teams that collected the samples used in this analysis, an effort unprecedented in oil spill investigations. The authors also wish to thank Nancy Rothman (New Horizons), William B. Driskell (Driskell Consultants), Ann Jones (Industrial Economics, Corp.) for coordinating the large analytical program, and Wendy Wong and Eric Litman (NewFields) who managed the chemical analysis conducted by the Alpha Analytical Laboratory staff.

Appendix A. Supplementary data

Supplementary data to this article can be found online at http://dx.doi.org/10.1016/j.marpolbul.2016.02.044.

References

Aeppli, C., Carmichael, C.A., Nelson, R.K., Lemkau, K.L., Graham, W.M., Redmond, M.C., Valentine, D.L., Reddy, C.M., 2012. Oil weathering after the Deepwater Horizon disaster led to the formation of oxygenated residues. Environ. Sci. Technol. 46 (16), 8799–8807.

Aeppli, C., Nelson, R.K., Radović, J.R., Carmichael, C.A., Valentine, D.L., Reddy, C.M., 2014. Recalcitrance and degradation of petroleum biomarkers upon abiotic and biotic natural. weathering of Deepwater Horizon oil. Environ. Sci. Technol. 48, 6726–6734.

Andersson, J.T., 1993. Polycyclic aromatic sulfur heterocycles III. Photochemical stability of the potential oil pollution markers phenanthrenes and dibenzothiophenes. Chemosphere 27, 2097–2102.

Bacosa, H., Erdner, D.L., Liu, Z., 2015. Differentiating the roles of photooxidation and biodegradation in the weathering of light Louisiana sweet crude oil in surface water from the Deepwater Horizon site. Mar. Pollut. Bull. 95, 265–272.

Camilli, R., Reddy, C.M., Yoerger, D.R., Van Mooy, B.A.S., Jakuba, M.V., Kinsey, J.C., McIntyre, C.P., Sylva, S.P., Maloney, J.V., 2010. Tracking hydrocarbon plume transport and biodegradation at Deepwater Horizon. Science 330, 201–204.

Carmichael, C.A., Arey, J.S., Graham, W.M., Linn, L.J., Lemkau, K.L., Nelson, R.K., Reddy, C.M., 2012. Floating oil-covered debris from Deepwater Horizon: indentification and application. Environ. Res. Lett. 7, 015301 (6 pp.).

CEN, 2012. Oil spill identification – Waterborne petroleum and petroleum products — part 2: analytical methodology and interpretation of results based upon GC-FID and GC–MS low resolution analysis. Center for European Norms Technical Report 15522-2 Oct. 3, 2012.

deGouw, J.A., Middlebrook, A.M., Warneke, C., Ahmadov, R., Atlas, E.L., Blake, C.A., Brock, C.A., Brioude, J., et al., 2011. Organic aerosol formation downwind from the Deepwater Horizon oil spill. Science 331 (6022), 1295–1299.

Douglas, G.S., Bence, A.E., Prince, R.C., McMillen, S.J., Butler, E.L., 1996. Environmental stability of selected petroleum source and weathering ratios. Environ. Sci. Technol. 30 (7), 2332–2339.

Douglas, G.S., Emsbo-Mattingly, S.D., Stout, S.A., Uhler, A.D., McCarthy, K.J., 2015. Hydrocarbon fingerprinting methods. In: Murphy, B.L., Morrison, R.D. (Eds.), Introduction to Environmental Forensics, third ed. Academic Press, Boston, pp. 201–309.

Edwards, B.R., Reddy, C.M., Camilli, R., Carmichael, C.A., Longnecker, K., Van Mooy, B.A.S., 2011. Rapid microbial respiration of oil from the Deepwater Horizon oil spill offshore surface waters of the Gulf of Mexico. Environ. Res. Lett. 6 (3), 035301.

Elmendorf, D.L., Haith, C.E., Douglas, G.S., Prince, R.C., 1994. Relative rates of biodegradation of substituted polycyclic aromatic hydrocarbons. In: Hinchee, R.E.L., A.E., Semprini, L., Ong, S.K. (Eds.), Bioremediation of Chlorinated and PAH Compounds. Lewis Publishers, Ann Arbor, Michigan, pp. 188–202.

Faksness, L.G., Altin, D., Nordtug, T., Daling, P.S., Hansen, B.H., 2015. Chemical comparison and acute toxicity of water accommodated fraction (WAF) of source and field collected Macondo oils from the Deepwater Horizon oil spill. Mar. Pollut. Bull. 91, 222–229.

Fingas, M., 1994. Evaporation of Oil Spills. J. ASCE.

Garrett, R.M., Pickering, I.J., Haith, C.E., Prince, R.C., 1998. Photooxidation of crude oils. Environ. Sci. Technol. 32 (23), 3719–3723.

Hall, G.J., Frysinger, G.S., Aeppli, C., Carmichael, C.A., Gros, J., Lemkau, K.L., Nelson, R.K., Reddy, C.M., 2013. Oxygenated weathering products of Deepwater Horizon oil come from surprising precursors. Mar. Pollut. Bull. 75, 140–149.

Hazen, T.C., Dubinsky, E.A., DeSantis, T.Z., Andersen, G.L., Piceno, Y.M., Singh, N., Jansson, J.K., Probst, A., Borglin, S.E., Fortney, J.L., Stringfellow, W.T., Bill, M., Conrad, M.E., Tom, L.M., Chavarria, K.L., Alusi, T.R., Lamendella, R., Joyner, D.C., Spier, C., Baelum, J., Auer, M., Zemla, M.L., Chakraborty, R., Sonnenthal, E.L., D'haeseleer, P., Holman, H.Y.N., Osman, S., Lu, Z., Van Nostrand, J.D., Deng, Y., Zhou, J., Mason, O.U., 2010. Deep sea oil plume enriches indigenous oil degrading bacteria. Science 330, 204–208.

Jordan, R.E., Payne, J.R., 1980. Fate and Weathering of Petroleum Spills in the Marine Environment. Ann Arbor Science Publ., Inc., Ann Arbor, MI.

King, S.M., Leaf, P.A., Olson, A.C., Ray, P.Z., Tarr, M.A., 2014. Photolytic and photocatalytic degradation of surface oil from the Deepwater Horizon spill. Chemosphere 95, 415–422.

Kiruri, L.W., Dellinger, B., Lomnicki, S., 2013. Tar balls from Deep Water Horizon oil spill: environmentally persistent free radicals (EPFR) formation during crude weathering. Environ. Sci. Technol. 47 (9), 4220–4226.

Lee, R.F., 2003. Photooxidation and phototoxicity of crude and refined oils. Spill Sci. Technol. Bull. 8, 157–162.
Lewan, M.D., Warden, A., Dias, R.F., Lowry, Z.K., Hannah, T.L., Lillis, P.G., Kokaly, R.F., Hoefen, T.M., Swayze, G.A., Mills, C.T., Harris, S.H., Plumlee, G.S., 2014. Asphaltene content and composition as a measure of Deepwater Horizon oil spill losses within the first 80 days. Org. Geochem. 75, 54–60.
Liu, Z.F., Liu, J.Q., Zhu, Q.Z., Wu, W., 2012. The weathering of oil after the Deepwater Horizon oil spill: insights from the chemical composition of the oil from the sea surface, salt marshes and sediments. Environ. Res. Lett. 7. http://dx.doi.org/10.1088/1748-9326/7/3/035302 (14 pp.).
Maki, H., Sasaki, T., Harayama, S., 2001. Photo-oxidation of biodegraded crude oil and toxicity of the photo-oxidized products. Chemosphere 44, 1145–2115.
McKenna, A.M., Nelson, R.K., Reddy, C.M., Savory, J.J., Kaiser, N.K., Fitzsimmons, J.E., Marshall, A.G., Rodgers, R.P., 2013. Expansion of the analytical window for oil spill characterization by ultrahigh resolution mass spectrometry: beyond gas chromatography. Environ. Sci. Technol. 47, 7530–7539.
Michel, J., Owens, E.H., Zengel, S., Graham, A., Nixon, Z., Allard, T., Holton, W., Reimer, P.D., Lamarche, A., White, M., Rutherford, N., Childs, C., Mauseth, G., Challenger, G., Taylor, E., 2013. Extent and degree of shoreline oiling: Deepwater Horizon oil spill, Gulf of Mexico, USA. PLoS One 8 (6), e65087.
NIOSH, 2010. Deepwater Horizon Response NIOSH Health Harzard Evaluation Interim Reports #1–8. National Institute of Occupational Health and Science, Atlanta (http://www.cdc.gov/niosh/topics/oilspillresponse/gulfspillhe.html. Accessed June 2011).
Operational Science Advisory Team (OSAT), Feb. 10, 2011. Summary report for fate and effects of remnant oil in the beach environment. Report to Federal On-Scene Coordinator, p. 64.
Payne, J.R., Driskell, W.B., 2015a. 2010 DWH offshore water column samples—forensic assessments and oil exposures. U.S. Dept. of Interior, Deepwater Horizon Response & Restoration, Admin. Record (www.doi.gov/deepwaterhorizon/adminrecord, DWH-AR0039118, 37 pp.).
Payne, J.R., Driskell, W.B., 2015b. Dispersant effects on waterborne oil profiles and behavior during the Deepwater Horizon oil spill. U.S. Dept. of Interior, Deepwater Horizon Response & Restoration, Admin. Record (www.doi.gov/deepwaterhorizon/adminrecord, DWH-AR0039201, 22 pp.).
Payne, J.R., McNabb Jr., G.D., 1984. Weathering of petroleum in the marine environment. Mar. Technol. Soc. J. 18 (3), 24–42.
Payne, J.R., Flynn, N.W., Mankiewicz, P.J., Smith, G.S., 1980. Surface evaporation/dissolution partitioning of lower-molecular-weight aromatic hydrocarbons in a downplume transect from the IXTOC I wellhead. Proceedings: Symposium on Preliminary Results from the September 1979 RESEARCHER/PIERCE IXTOC I Cruise, pp. 239–263 (June 9–10, 1980, Key Biscayne, Florida. NTIS Accession Number PB-246068).
Plata, D.L., Sharpless, C.M., Reddy, C.M., 2008. Photochemical degradation of polycyclic aromatic hydrocarbons in oil films. Environ. Sci. Technol. 42, 2432–2438.
Prince, R.C., Elmendorf, D.L., Lute, J.R., Hsu, C.S., Haith, C.E., Senius, J.D., Dechert, G.J., Douglas, G.S., Butler, E.L., 1994. 17α(H),21β(H)-hopane as a conserved internal marker for estimating the biodegradation of crude oil. Environ. Sci. Technol. 28 (1), 142–145.
Prince, R.C., Stibrany, R.T., Hardenstine, J., Douglas, G.S., Owens, E.H., 2002. Aqueous vapor extraction: a previously unrecognized weathering process affecting oil spills in vigorously aerated water. Environ. Sci. Technol. 36 (13) (2833–2825).
Prince, R.C., Garrett, R.M., Bare, R.E., Grossman, M.J., Townsend, T., Suflita, J.M., Lees, K., Owens, E.H., Sergy, G.A., Braddocks, J.F., Lindstrom, J.E., Lessard, R.R., 2003. The roles of photooxidation and biodegradation in long-term weathering of crude and heavy fuel oils. Spill Sci. Technol. Bull. 8 (2), 145–156.
Prince, R.C., McFarlin, K.M., Butler, J.D., Febbo, E.J., Wang, F.C.Y., Nedwed, T.J., 2013. The primary biodegradation of dispersed crude oil in the sea. Chemosphere 90, 521–526.
Radović, J.R., Aeppli, C., Nelson, R.K., Jimenez, N., Reddy, C.M., Bayona, J.M., Albaigés, J., 2014. Assessment of photochemical processes in marine oil spill fingerprinting. Mar. Pollut. Bull. 79, 268–277.
Ramseur, J.L., 2010. Deepwater Horizon oil spill: the fate of the oil. Congressional. Research Service Report 7-5700, Dec. 16.
Reddy, C.M., Arey, J.S., Seewald, J.S., Sylva, S.P., Lemkau, K.L., Nelson, R.K., Carmichael, C.A., McIntyre, C.P., Fenwick, J., Ventura, G.T., Van Mooy, B.A.S., Camilli, R., 2012. Composition and fate of gas and oil released to the water column during the Deepwater Horizon oil spill. Proc. Natl. Acad. Sci. 109 (50), 20229–20234.
Ruddy, B.M., Huettel, M., Kostka, J.E., Lobodin, V.V., Bythell, B.J., McKenna, A.M., Aeppli, C., Reddy, C.M., Nelson, R.K., Marshall, A.G., Rodgers, R.P., 2014. Targeted petroleomics: analytical investigation of Macondo well oil oxidation products from Pensacola Beach. Energy Fuel 28, 4043–4050.
Ryerson, T.B., Camilli, R., Kessler, J.D., Kujawinski, E.B., Reddy, C.M., Valentine, D.L., Atlas, E., Blake, D.R., de Gouw, J., Meinardi, S., Parrish, D.D., Peischl, J., Seewald, J.S., Warneke, C., 2012. Chemical data quantify Deepwater Horizon hydrocarbon flow rate and environmental distribution. Proc. Natl. Acad. Sci. 109 (50), 20246–20253.
Villalanti, D.C., Raia, J.C., Maynard, J.B., 2000. High-temperature simulated distillation applications. In: Meyers, R.A. (Ed.), Petroleum Characterization in Encyclopedia of Analytical Chemistry. J. Wiley & Sons Ltd., Chichester, UK, pp. 6726–6741.
Wang, Z., Stout, S.A., Fingas, M., 2006. Forensic fingerprinting of biomarkers for oil spill characterization and source identification. Environ. Forensic 7 (2), 105–146.